SIMULATION OF VEHICLE IMPACT WITH THE TEXAS CONCRETE MEDIAN BARRIER VOLUME I: TEST COMPARISONS AND PARAMETER STUDY

by

Ronald D. Young
Engineering Research Associate

Edward R. Post
Assistant Research Engineer

Hayes E. Ross, Jr.
Associate Research Engineer

and

Robert M. Holcomb
Graduate Research Assistant

Research Report 140-5
Volume I

Evaluation of the Roadway Environment by
Dynamic Analysis of the Interaction Between
the Vehicle, Passenger, and Roadway

Research Study No. 2-5-69-140

Sponsored by
The Texas Highway Department

in cooperation with the
U.S.Department of Transportation, Federal Highway Administration

June 1972

TEXAS TRANSPORTATION INSTITUTE
Texas A&M University
College Station, Texas

FOREWORD

The information contained herein was developed on Research Project 2-5-69-140 entitled "Evaluation of the Roadside Environment by Dynamic Analysis of the Interaction Between the Vehicle, Passenger, and Roadway" which is a cooperative research study sponsored jointly by the Texas Highway Department and the U. S. Department of Transportation, Federal Highway Administration.

Basically, the objectives of the study are to apply mathematical simulation techniques in determining the dynamic behavior of automobiles and their occupants when in collision with various roadside objects or when traversing curves in the road, shoulders, or other situations. It is a continuing study, having been initiated in September 1968.

As part of the first year's work, the computer program HVOSM (formerly known as CALSVA) was obtained from Cornell Aeronautical Laboratory and made operational on the IBM 360 computer facilities at Texas A&M University. In adapting the program, additions and modifications were made which increased its flexibility and usefulness. These changes and the input requirements of the program are documented in Research Report 140-1.

The primary emphasis of the second year's work was the development of an analytical model which predicts the dynamic response of an automobile's occupant in three-dimensional space. Research Report 140-2 presents the derivation of the occupant model, a validation study, and a description of computer input data for determining the occupant's response.

In the 1970-71 year the emphasis was on application of HVOSM to specific roadway design problems. Research Report 140-3 describes an investigation of the *traffic-safe* characteristics of different sloping culvert grate configurations. Criteria are presented for designing a *traffic-safe* sloping grate. Research Report 140-4 describes the development of criteria from which the need and location of guardrail on embankments can be determined.

Volume I of this report describes a comparison of full-scale test results of the Texas Concrete Median Barrier with simulated results as computed by a modified version of HVOSM. Also contained in Volume I is a parametric study of the performance characteristics of the CMB for various vehicle encroachment or impact conditions. Volume II contains the computer input for all runs made and some sample output.

The contents of this report reflect the views of the authors who are responsible for the facts and the accuracy of the data presented herein. The contents do not necessarily reflect the official views or policies of the Federal Highway Administration. This report does not constitute a standard, specification, or regulation.

ABSTRACT

Key Words: Accidents, Automobile, Barrier Impact, Computer Simulation, Concrete Median Barrier, Injury Level, Math Modeling, Safety, Severity Index, Vehicle Redirection, Vehicle Simulation

The Highway-Vehicle-Object Simulation Model (HVOSM), a computer program developed at Cornell Aeronautical Lab. (CAL), has been modified with generous help from CAL and used to successfully simulate a vehicle impacting the Texas Concrete Median Barrier (CMB) at speeds ranging from 50 to 80 m.p.h. and angles ranging from 5 to 25 degrees.

The Texas CMB (a New Jersey type design) was impacted by a 4000 lb. sedan at angles of 7, 15 and 25 degrees at 60 m.p.h. The results of these full scale tests were closely approximated by the modified HVOSM.

Comparison of simulation and test results are presented both visually and quantitatively in the form of computer generated drawings of the vehicle during impact alongside corresponding frames from the high speed film and plots relating predicted and measured accelerometer readings.

Following the successful simulation of the full scale tests, a parameter study on impact conditions was conducted. Using the modified HVOSM, a 4780 lb. vehicle impacting the CMB was simulated for speeds of 50, 70 and 80 m.p.h. at angles of 5, 10 and 15 degrees for each of those speeds.

For speeds less than 70 m.p.h., the results were in line with

findings of other researchers in testing similar barriers. However, it was concluded that for impact speeds of 70 m.p.h. and greater in conjunction with impact angles of 15 degrees and greater, automobile rollover can be expected.

The results of all simulated impacts with the Texas CMB are presented graphically with regard to a severity index which quantifies the severity of each crash. This index is based on vehicle accelerations.

SUMMARY

In this study, the performance of the Texas Concrete Median Barrier (CMB) was evaluated from the standpoint of severity of impact, vehicle exit angle, maximum roll angle, and maximum pitch angle for a wide range of vehicle encroachment conditions. A modified version of the Highway-Vehicle-Object Simulation Model (HVOSM) was used to simulate a 4780 lb. automobile impacting the CMB at speeds of 50, 70, and 80 m.p.h. at angles of 5, 10 and 15 degrees for each of those speeds. These parameter studies were preceded by a validation phase where full-scale tests on the CMB were successfully simulated with the HVOSM.

In summary the major findings are:

1. that the Texas CMB performs well with respect to exit angle and maximum roll and pitch angles at least up to 80 m.p.h. (highest speed considered) for impact angles of less than 10 degrees.
2. that serious injuries could occur at 70 m.p.h. for impact angles greater than 7.5 degrees (see Figure 25).
3. that rollover can be expected for speeds greater than 70 m.p.h. at angles greater than 15 degrees. Although these encroachment conditions would probably result in serious or fatal injury even without the rollover, this creates a hazard for other motorists as well.

IMPLEMENTATION STATEMENT

There is very little disagreement (if any) among Highway Engineers on the superior attributes of the Concrete Median Barrier (New Jersey or Texas type) for use in narrow medians of roadways carrying high traffic volume such as in urban areas. Tests have shown that impacting the CMB at low angles is safe and that maintenance is virtually non existant.

The results of this study provide additional detailed information which will aid the highway designer in evaluating an existing roadway for possible installation of a CMB or designing a new roadway to accomodate a CMB. For an automobile colliding with the Texas CMB, Figure 25 of this report gives combinations of speed and impact angles for which serious injury to the occupant is unlikely.

ACKNOWLEDGEMENTS

This research was sponsored by the Texas Highway Department (THD) in cooperation with the U.S. Department of Transportation, Federal Highway Administration(FHWA).

The authors sincerely thank Messrs. Norman J. Deleys and Raymond R. McHenry of Cornell Aeronautical Laboratories for providing generous professional assistance in the form of copies of their previous work on modifying their model, the Highway-Vehicle-Object Simulation Model (HVOSM), to include the effect of vehicle structural hard points in similating automobile-barrier crashes.

Thanks are also extended to Messrs. John F. Nixon and David Hustace (THD) and Mr. Edward V. Kristaponis (FHWA) for their cooperation in meeting the uncertainties of this particular research effort and their patience in awaiting the reported results.

TABLE OF CONTENTS

LIST OF FIGURES

LIST OF FIGURES (CONTINUED)

LIST OF TABLES

I. INTRODUCTION

Evaluation of barrier systems usually include full-scale vehicle crash tests. These tests are often quite expensive and many man-hours are required for all phases of the test program. A more ideal method of studying the performance of barriers is by computer simulation.

The original version of the Highway-Vehicle-Object-Simulation Model (HVOSM)* (1,2) was capable of predicting automobile behavior for impact with certain types of barriers, provided the automobile crush was moderate (12 to 18 inches). The types of barrier systems which can be studied with the HVOSM are those whose lateral resistance to vehicle penetration is independent of the longitudinal position of the vehicle contact. The Texas Highway Department (THD) concrete median barrier (CMB), being a rigid barrier, falls within this category. To study barrier impacts in which large automobile crush occurs, the HVOSM was modified to include *hard points* within the automobile structure. These hard points simulate the effects caused when very stiff automobile members are encountered, such as the engine, a frame member, or a wheel assembly. Basic details of HVOSM are summarized in Appendix A and a description of the hard point modifications is given in Appendix B.

In Chapter II, comparisons are made between experimental data from full-scale crash tests of the Texas CMB and simulated results from TTI's modified version of HVOSM (including hard points). The

---

*Formerly known as CALSVA.

crash test data were obtained from another THD sponsored research program (3). In general, good correlation exists between simulated and experimental results.

A parametric study of the Texas concrete median barrier was conducted using HVOSM and the results are described in Chapter III. The parametric study was used to determine the barrier's performance characteristics for a range of vehicle encroachment conditions. Factors used in measuring the performance were the vehicle's exit angle, maximum pitch and roll angle, and a severity index which quantified the impact severity.

II. COMPARISON OF EXPERIMENTAL DATA WITH PREDICTIONS BY HVOSM

General

It was felt by sponsors and researchers alike that a good correlation between simulation and testing was a prerequisite to conducting parametric studies of the Texas CMB with the HVOSM. The crash test data used in the comparisons were obtained from another THD sponsored research program (3) and the results were available to this study at no extra cost.

The three tests used in the comparisons consisted of passenger cars (roughly 4000 lbs. in weight) being towed into a full scale model of the CMB, model I-70 (designated CMBI-70), at approximately 60 mph for impact angles of 7, 15, and 25 degrees. The CMBI-70 designation is used when illumination poles are placed atop the barrier. The exterior dimensions of the barrier are the same however, whether illumination is used or not. Reference to the barrier will henceforth be the CMB. Accelerometers were mounted to the structural framework of the vehicles, at the locations described in APPENDIX C (Figures C1 and C2). They were oriented to measure the lateral and the longitudinal components of vehicle acceleration. Vehicle motion was recorded on high speed film from rear, side, and overhead views. These films were used to determine the automobile's speed and angle at impact and to provide a comparison of the vehicle's simulated and actual motion.

The computer simulation used was a modified version of the HVOSM, as discussed in Appendix B. The modification made was the addition of

NOTE: Dotted Outline Shows the Actual Shape of the CMBI-70 and Solid Lines Show the Shape Used for Simulation.

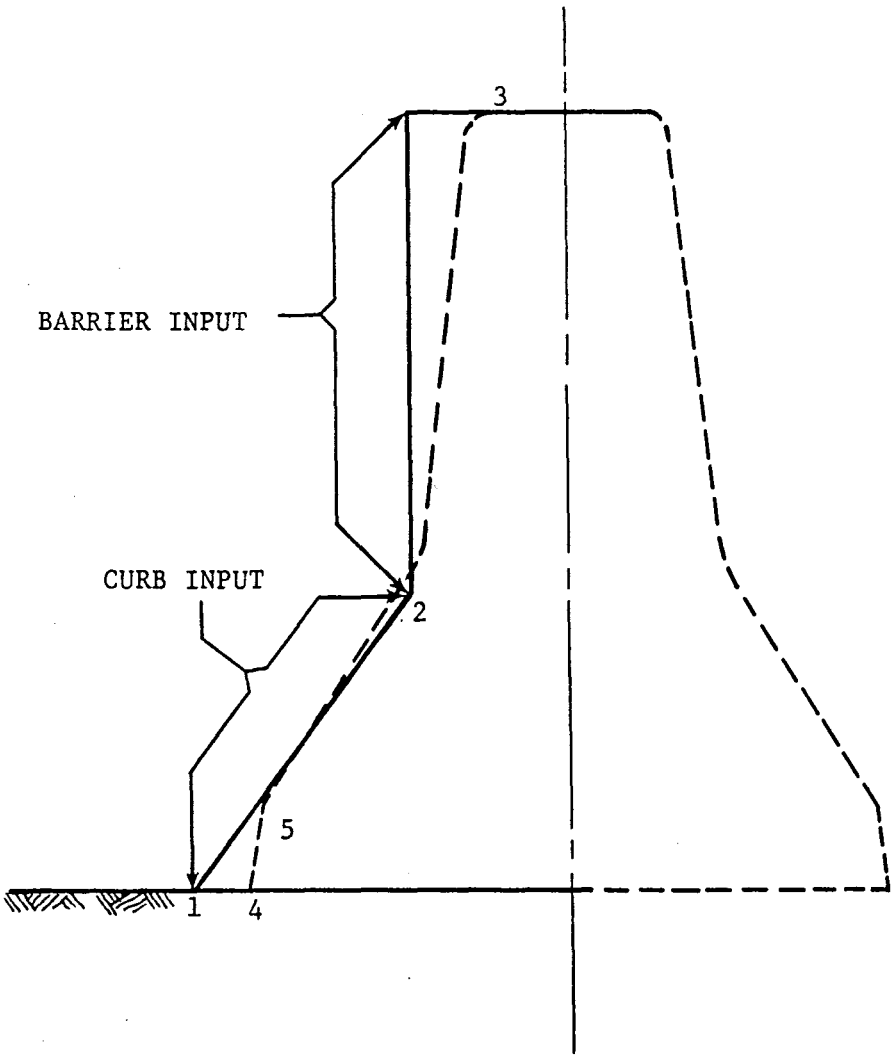

FIGURE 1. IDEALIZATION OF THE CMBI-70 FOR COMPUTER SIMULATION.

vehicle structural hard points to the existing sheet metal crushing capability, to account for stiffer portions of the vehicle (frame members, wheels, etc.) impacting the barrier.

Due to limitations within HVOSM, it was necessary to describe the CMB by a combination (or superposition) of the program's "curb impact" and "barrier impact" capabilities. As shown in Figure 1, the sloping face of the barrier was simulated as a curb (line 1-2) and the upright face was simulated as a vertical rigid barrier (line 2-3). In the simulation tire-curb interaction is accounted for but tire-rigid barrier interaction is not. However, since good comparisons between simulations and tests were obtained (for both kinematics and accelerations), it would appear that tire contact with the upright face is of secondary importance. For the same reason, the omission of slope 4-5 was apparently not detrimetal to the simulation. This is not surprising in view of the relative dimensions of the tires to the length of line 4-5 and the high impact speeds. Likewise, idealizing the upright face as vertical rather than sloped a few degrees proved to be an adequate representation. For the shallow angle impact of 7°, the whole concrete median barrier could have been defined as one high curb (1), but for the sake of uniformity all cases were defined as described above.

Data corresponding to the CMB and the test vehicles, such as vehicle weight, barrier and vehicle dimensions, impact speed and angle, etc., were read into the HVOSM program. All computer imput data are described in Volume II of this report (4).

Plots of the predicted and measured acceleration components at

points corresponding to the locations of accelerometers in the actual vehicle were made. Drawings of the simulated impacts were generated using a computer program (5). The program produces a perspective drawing of the vehicle and barrier at selected times, utilizing vehicle position as determined from the HVOSM. These line drawings were then compared with corresponding photographs taken from the high speed photography of the test.

Results of the Comparisons

The results of the comparisons are given both pictorially and graphically in Figures 2 through 23. It should be noted that the test results are for a vehicle impacting on the left (driver) side of the vehicle, while the simulation impacts the car on the opposite side (passenger side). For this reason, the results are expressed in terms of "impact side" and "free side" of the vehicle, the free side being the side of the vehicle away from the wall. Time of initial impact was taken as zero and the times shown on the figures are with respect to impact time. Comparisons were stopped when the vehicle lost contact with the barrier.

The comparison of test photographs to computer drawings in Figures 2 through 11 is very good for all three tests. Comparing the wheel positions, height of climb, and relative position of vehicle body to the ground shows that the simulation accurately computed the motions of the test vehicle. The small differences observable

TEST

SIMULATION

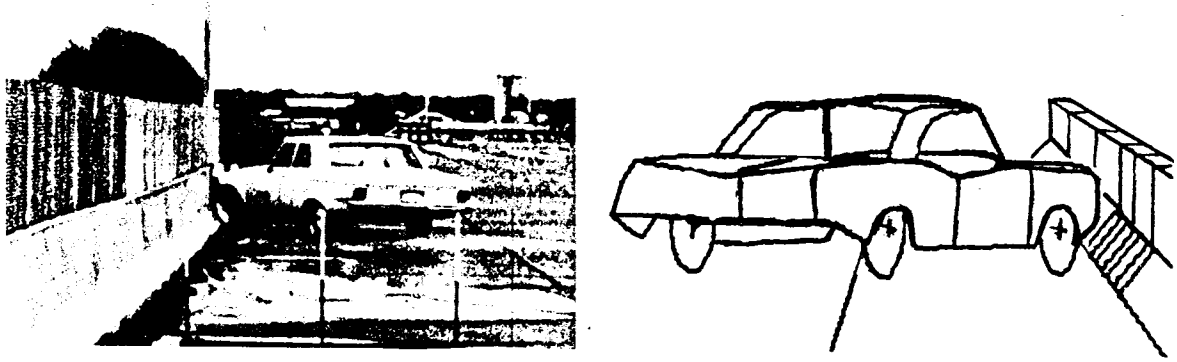

TIME = 0.000 SEC.

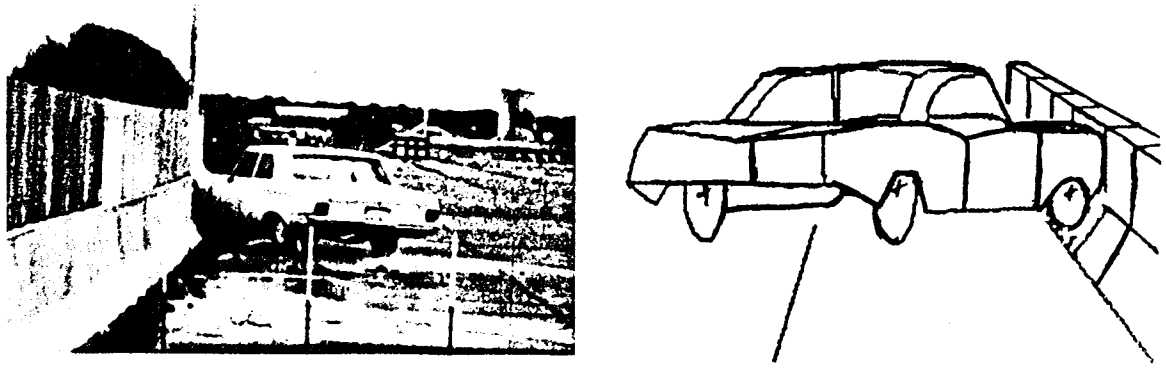

TIME = 0.035 SEC.

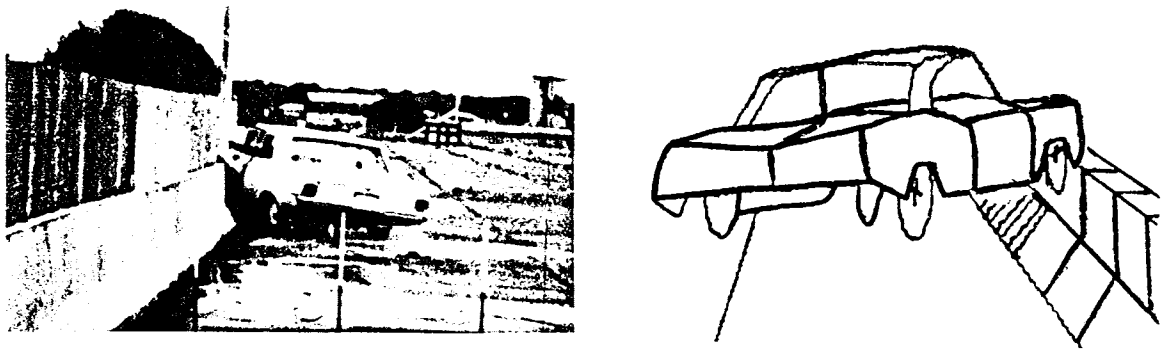

TIME = 0.085 SEC.

FIGURE 2.- COMPARISON OF COMPUTER SIMULATION WITH TEST RESULTS FOR 4000 LB. VEHICLE IMPACTING CONCRETE MEDIAN BARRIER AT 63 MPH AT 25 DEGREES; TIME = 0.000 SEC. TO 0.085 SEC.

TEST

SIMULATION

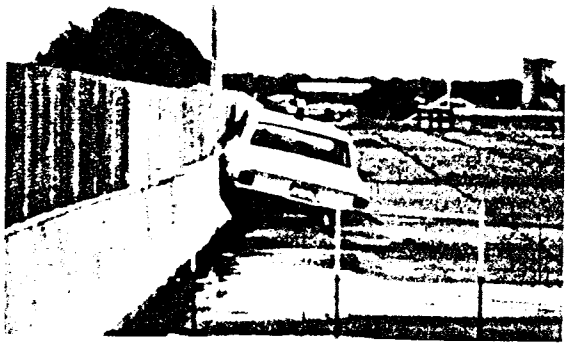

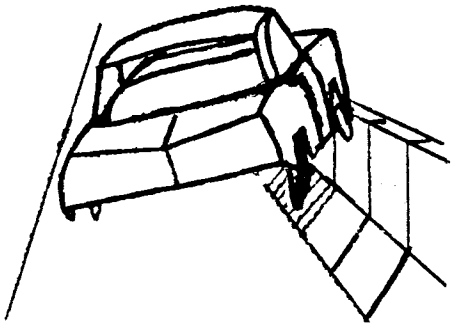

TIME = 0.156 SEC.

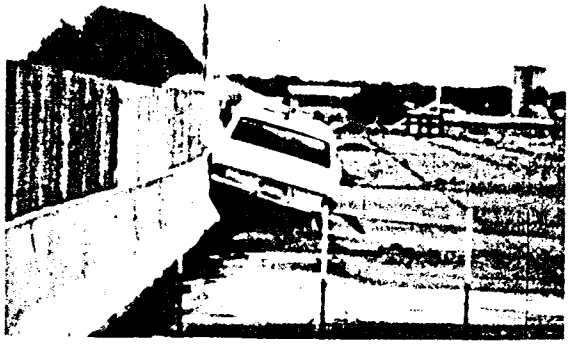

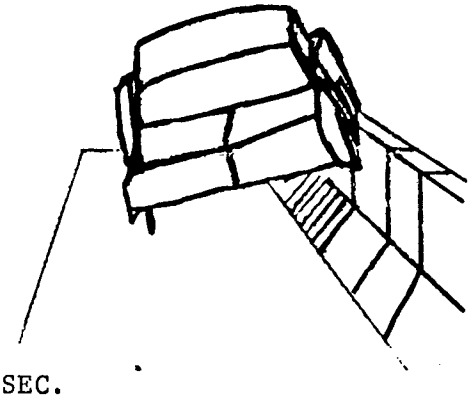

TIME = 0.201 SEC.

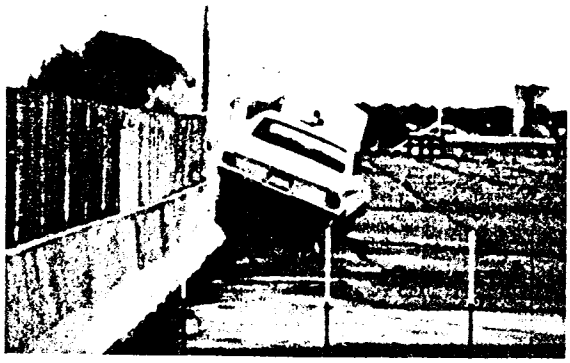

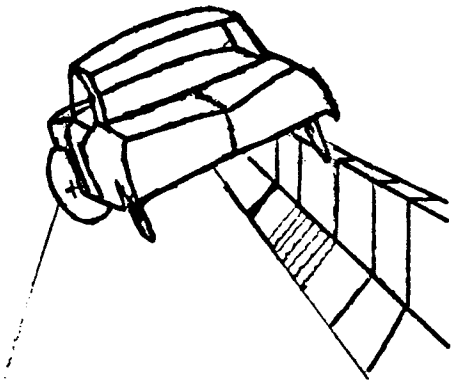

TIME = 0.321 SEC.

FIGURE 3. - COMPARISON OF COMPUTER SIMULATION WITH TEST RESULTS FOR 4000 LB. VEHICLE IMPACTING CONCRETE MEDIAN BARRIER AT 63 MPH AT 25 DEGREES; TIME = 0.156 SEC. TO 0.321 SEC.

TEST SIMULATION

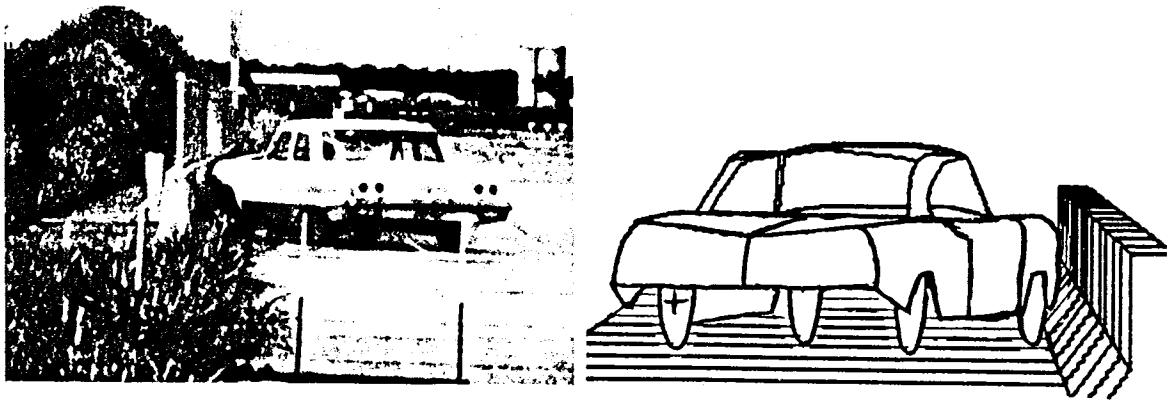

TIME = 0.000 SEC.

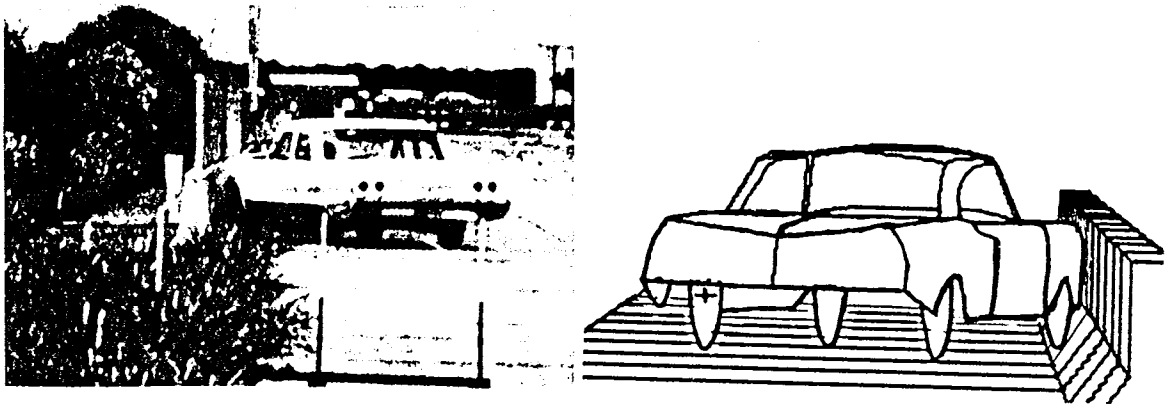

TIME = 0.035 SEC.

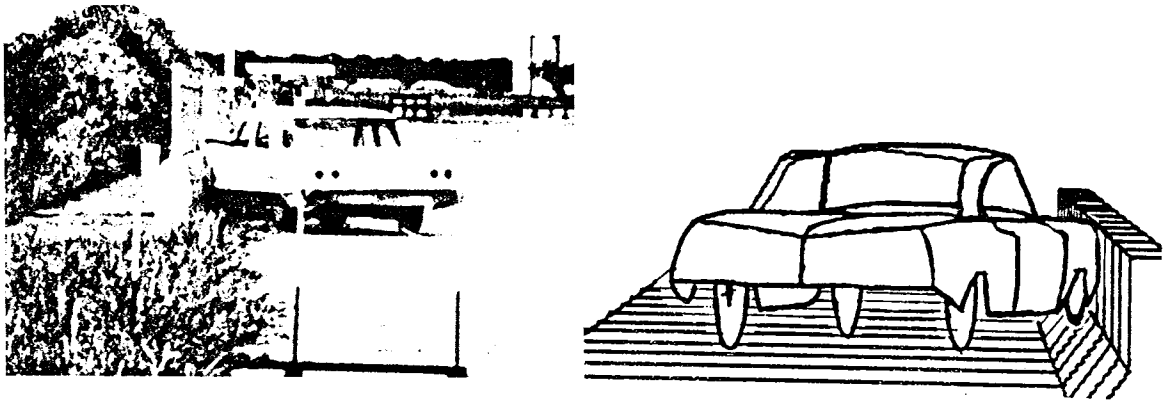

TIME = 0.06 SEC.

FIGURE 4.- COMPARISON OF COMPUTER SIMULATION WITH TEST RESULTS FOR 4210 LB. VEHICLE IMPACTING CONCRETE MEDIAN BARRIER AT 59.6 MPH AT 15 DEGREES; TIME = 0.000 SEC. TO 0.060 SEC.

TEST

SIMULATION

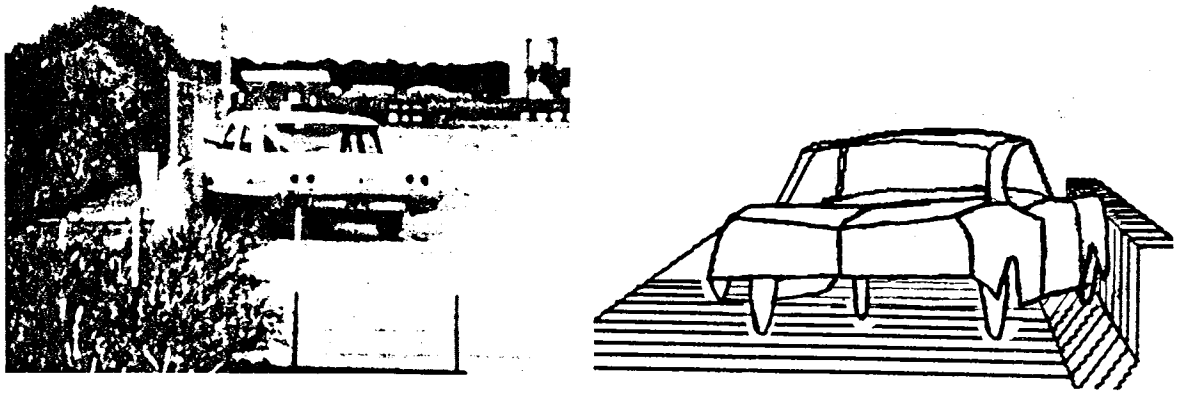

TIME = 0.085 SEC.

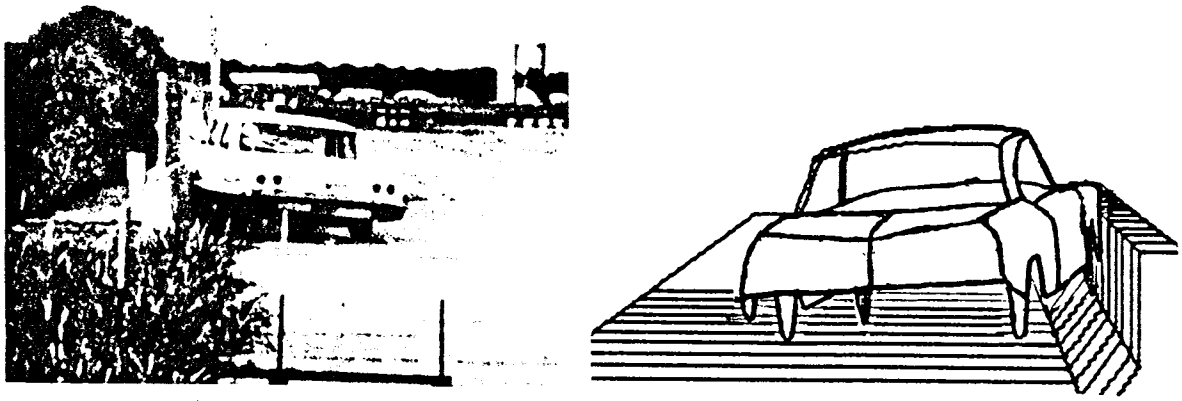

TIME = 0.110 SEC.

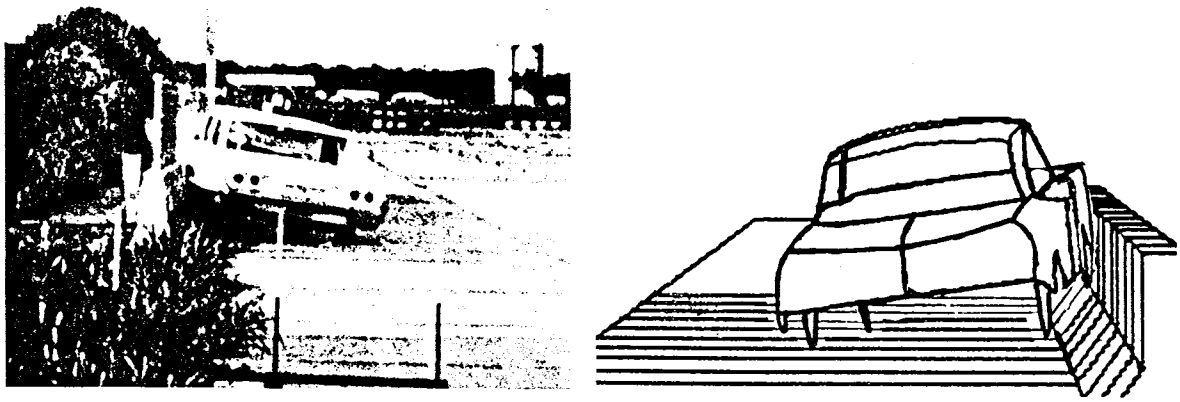

TIME = 0.135 SEC.

FIGURE 5.- COMPARISON OF COMPUTER SIMULATION WITH TEST RESULTS FOR 4210 LB. VEHICLE IMPACTING CONCRETE MEDIAN BARRIER AT 59.6 MPH AT 15 DEGREES; TIME = 0.085 SEC. TO 0.135 SEC.

TEST SIMULATION

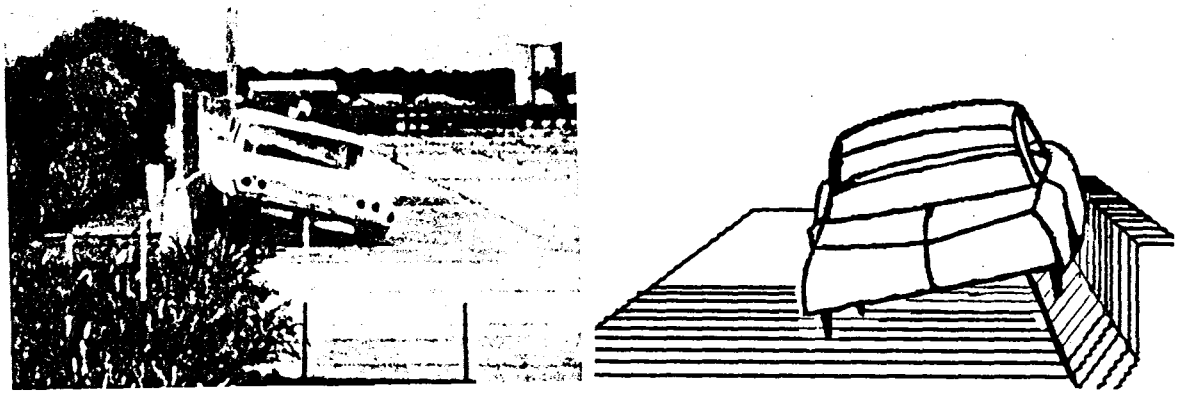

TIME = 0.160 SEC.

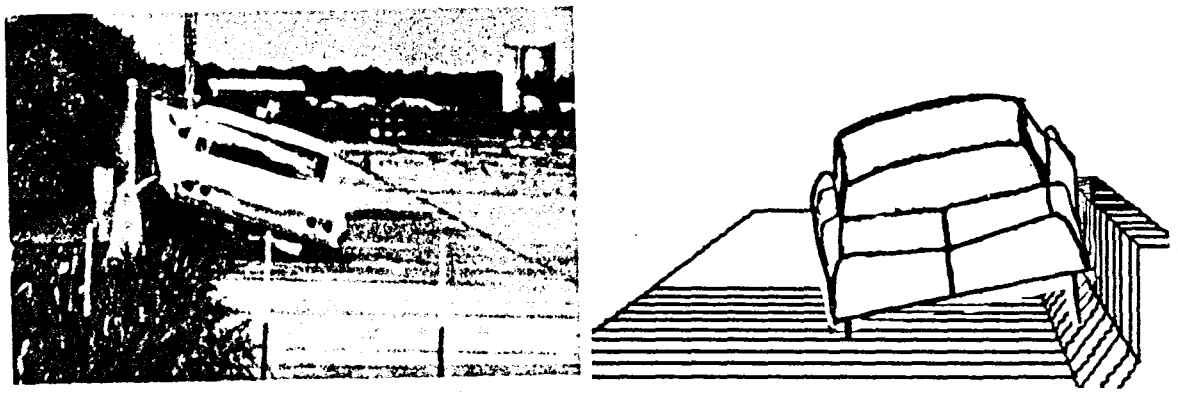

TIME = 0.185 SEC.

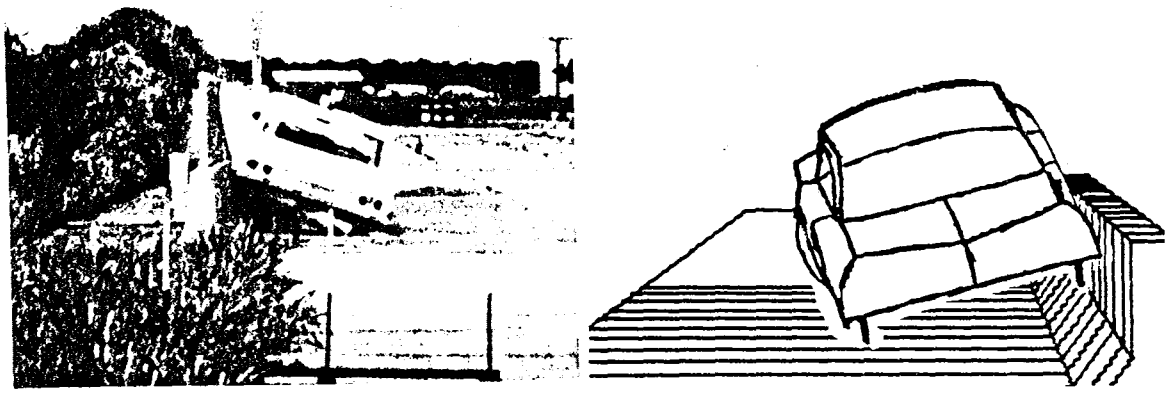

TIME = 0.210 SEC.

FIGURE 6.- COMPARISON OF COMPUTER SIMULATION WITH TEST RESULTS FOR 4210 LB. VEHICLE IMPACTING CONCRETE MEDIAN BARRIER AT 59.6 MPH AT 15 DEGREES; TIME = 0.160 SEC. TO 0.210 SEC.

TEST

SIMULATION

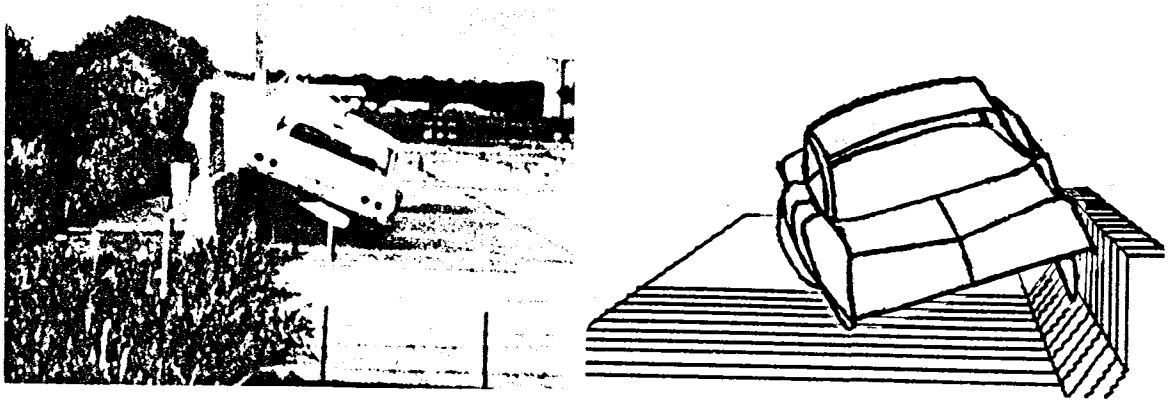

TIME = 0.285 SEC.

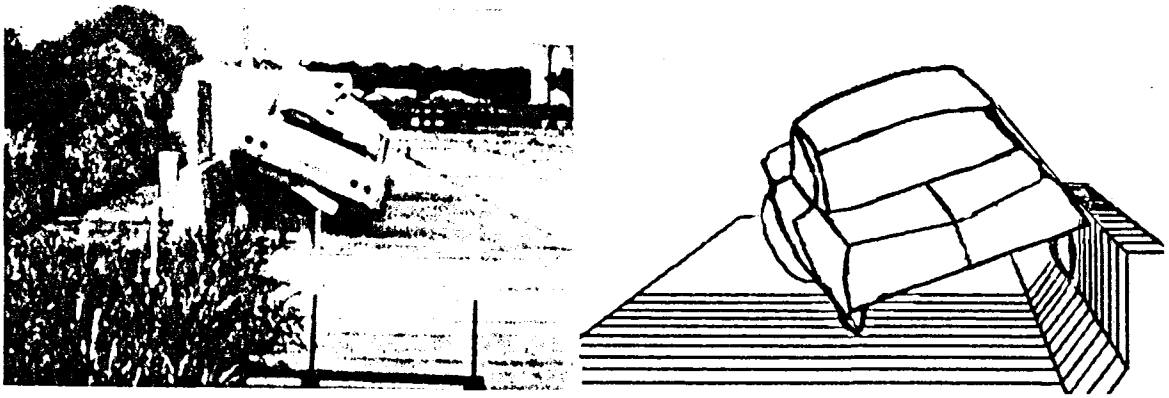

TIME = 0.335 SEC.

FIGURE 7.- COMPARISON OF COMPUTER SIMULATION WITH TEST RESULTS FOR 4210 LB. VEHICLE IMPACTING CONCRETE MEDIAN BARRIER AT 59.6 MPH AT 15 DEGREES; TIME = 0.285 SEC. TO 0.335 SEC.

TEST SIMULATION

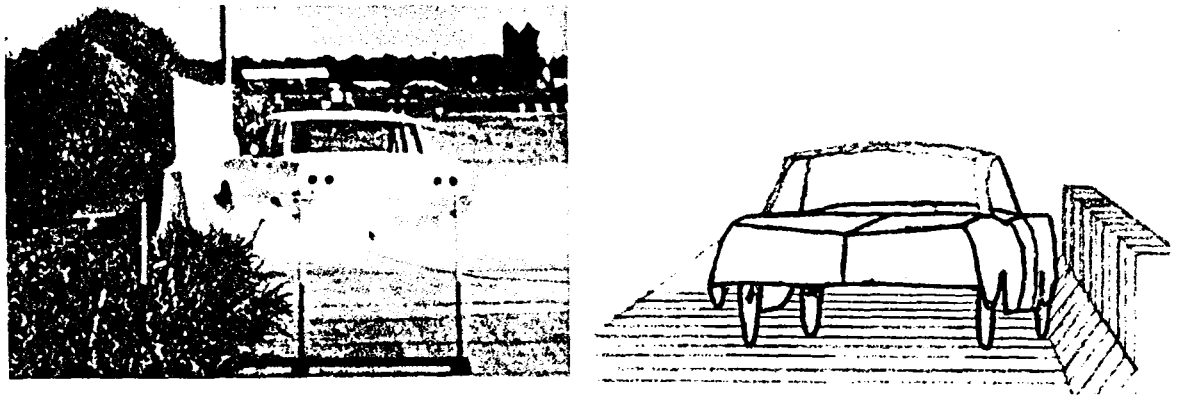

TIME = 0.000 sec.

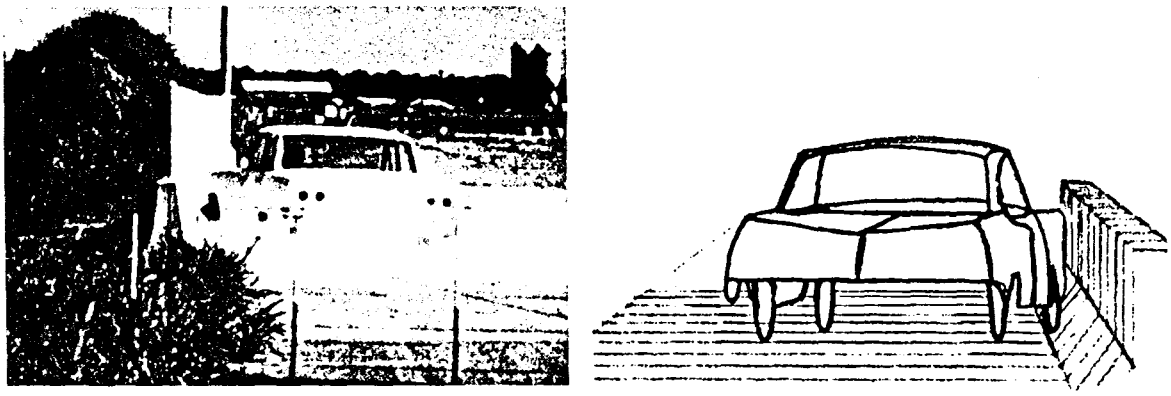

TIME = 0.025 sec.

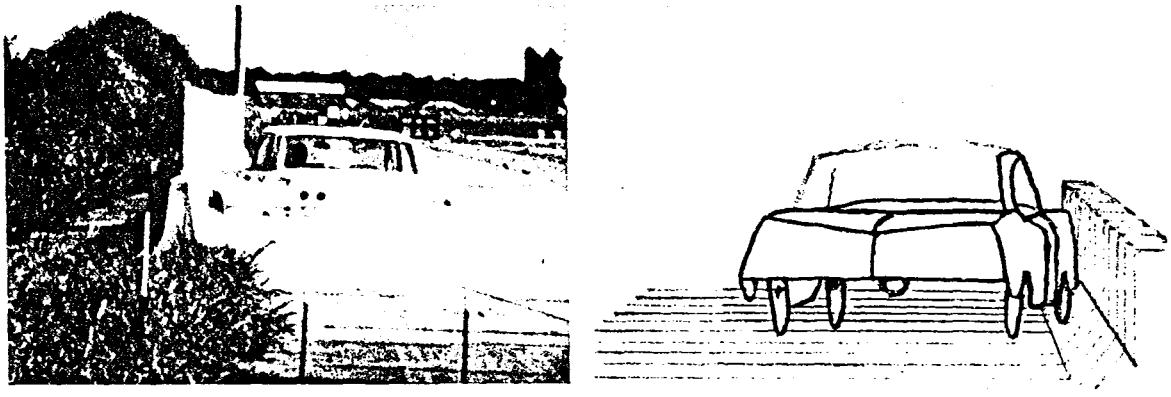

TIME = 0.050 sec.

FIGURE 8. - COMPARISON OF COMPUTER SIMULATION WITH TEST RESULTS FOR 4210 LB. VEHICLE IMPACTING CONCRETE MEDIAN BARRIER AT 61.9 MPH AT 7 DEGREE; TIME = 0.000 SEC. TO 0.050 SEC.

TEST

SIMULATION

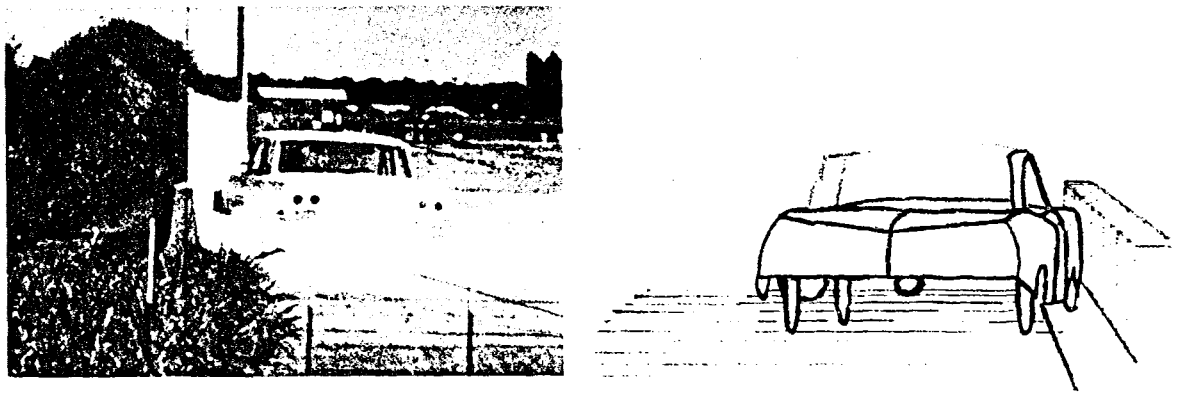

TIME = 0.075 SEC.

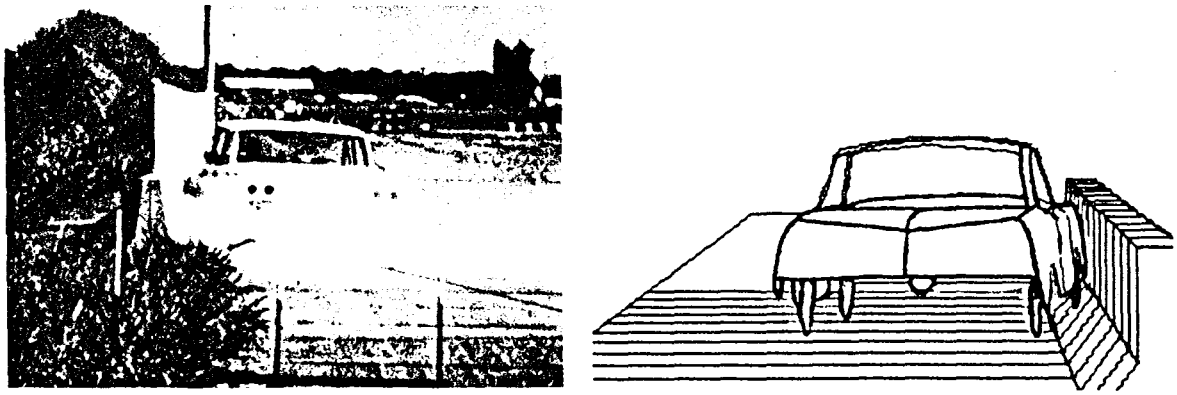

TIME = 0.100 SEC.

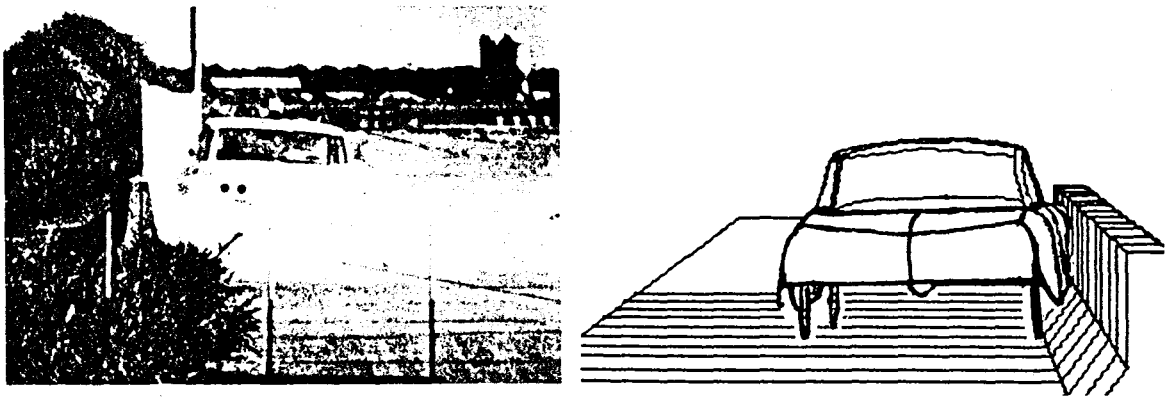

TIME = 0.125 SEC.

FIGURE 9. - COMPARISON OF COMPUTER SIMULATION WITH TEST RESULTS FOR 4210 LB. VEHICLE IMPACTING CONCRETE MEDIAN BARRIER AT 61.9 MPH AT 7 DEGREES; TIME = 0.075 SEC. TO 0.125 SEC.

TEST SIMULATION

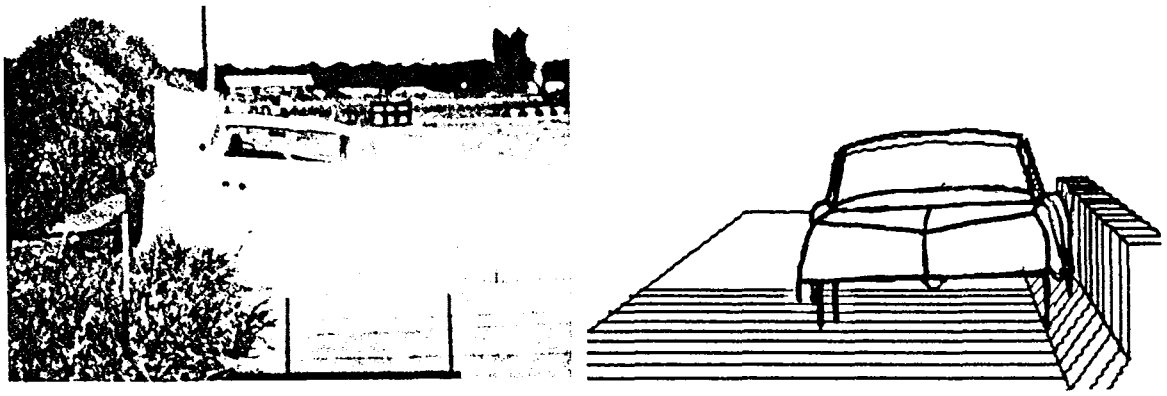

TIME = 0.150 SEC.

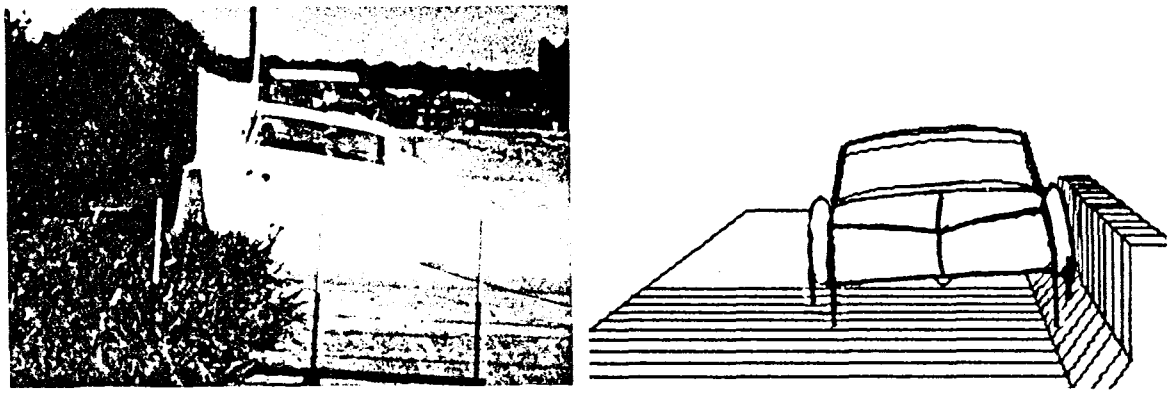

TIME = 0.175 SEC.

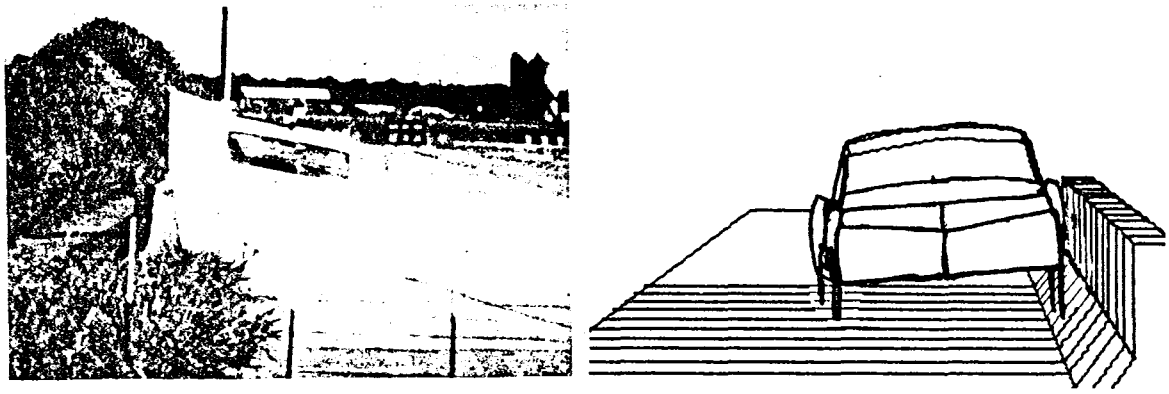

TIME = 0.200 SEC.

FIGURE 10- COMPARISON OF COMPUTER SIMULATION WITH TEST RESULTS FOR 4210 LB. VEHICLE IMPACTING CONCRETE MEDIAN BARRIER AT 61.9 MPH AT 7 DEGREES; TIME = 0.150 SEC. TO 0.200 SEC.

TEST SIMULATION

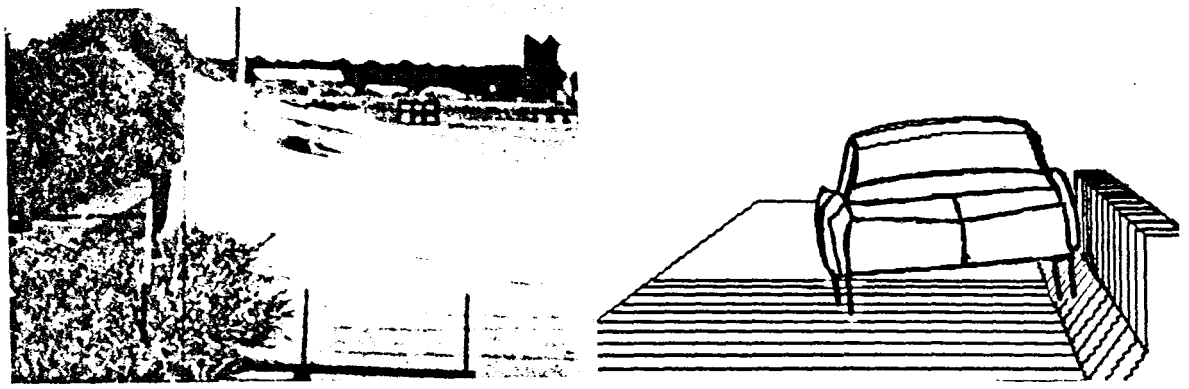

TIME = 0.225 SEC.

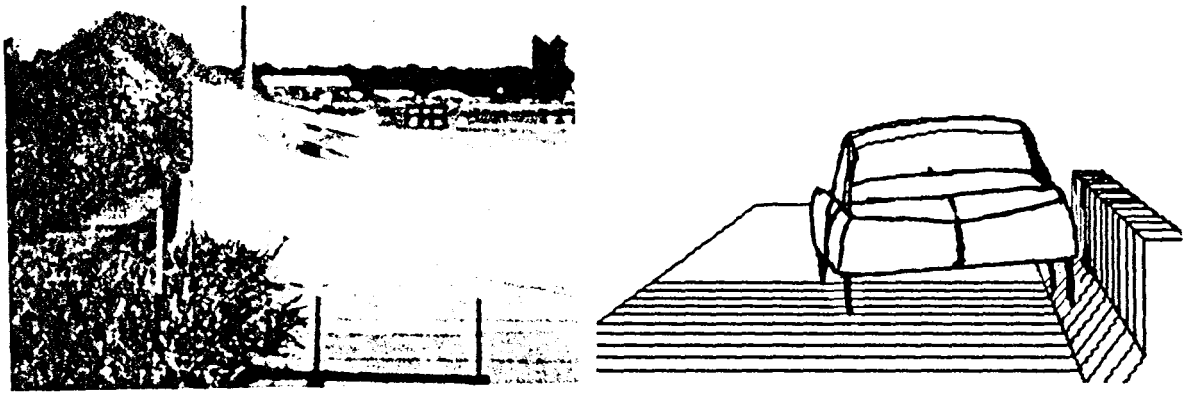

TIME = 0.250 SEC.

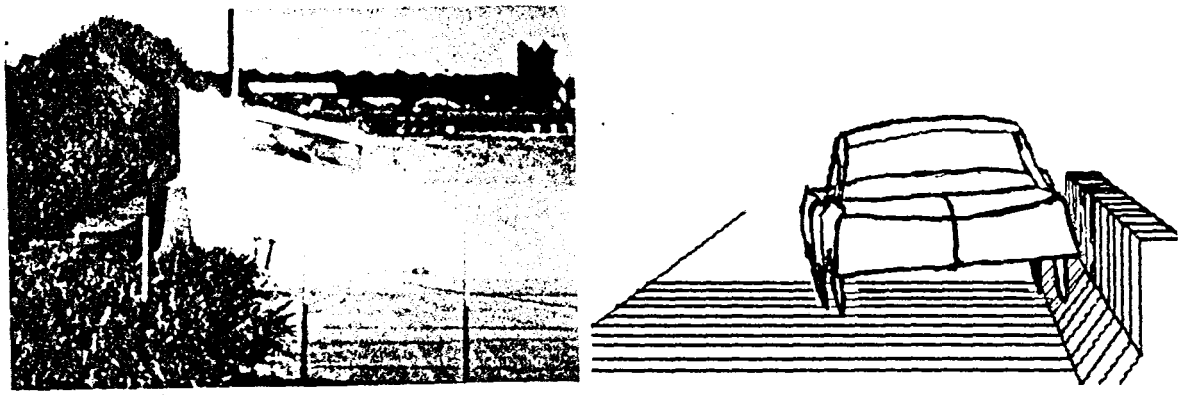

TIME = 0.275 SEC.

FIGURE 11.- COMPARISON OF COMPUTER SIMULATION WITH TEST RESULTS FOR 4210 LB. VEHICLE IMPACTING CONCRETE MEDIAN BARRIER AT 61.9 MPH AT 7 DEGREES; TIME = 0.225 SEC. TO 0.275 SEC.

between the positions of simulated and actual vehicles is largely attributable to a standard automobile used for all the computer drawings, which was not necessarily of the same dimensions as the actual test vehicles. A second noticeable discrepancy is the appearance of the simulated vehicle to penetrate the barrier in a few instances. The program which produces the computer drawing cannot show sheet metal crushing, although it is accounted for in the HVOSM.

The comparisons of simulated and measured acceleration components are given in Figures 12 through 15 for the 63 mph and 25 degree impact and in Figure 16 through 19 for the 59.6 mph and 15 degree impact. Taken at face value, these two comparisons could be considered good, whereas the comparison of accelerations for the 61.9 mph and 7 degree impact (Figures 20 through 23) could only be considered poor. Fortunately, the discrepancies occurring in all three cases, whether slight or major, can be explained in terms of two basic differences between the actual and simulated vehicles:

1. The actual vehicle structure is comprised of structural subassemblies each possessing its own vibrational characteristics (natural frequencies and damping). However, the simulated vehicle structure (wheels and suspension systems excluded) is a rigid mass which is undamped and free of natural frequencies of vibration. Therefore, the actual accelerometers will respond to those structural vibrations which do not contribute to vehicle redirection and accordingly, which

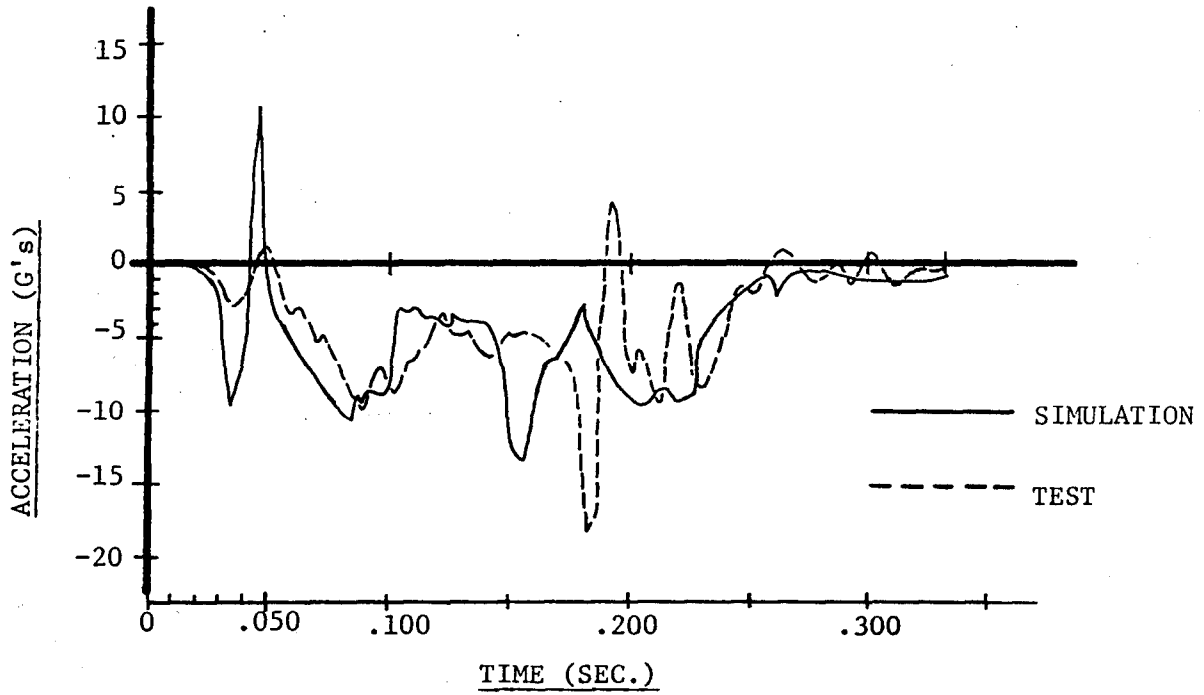

FIGURE 12.- LATERAL ACCELERATION ON IMPACT SIDE OF 4000 LB. VEHICLE IMPACTING CONCRETE MEDIAN BARRIER AT 63 MPH AT 25 DEGREES.

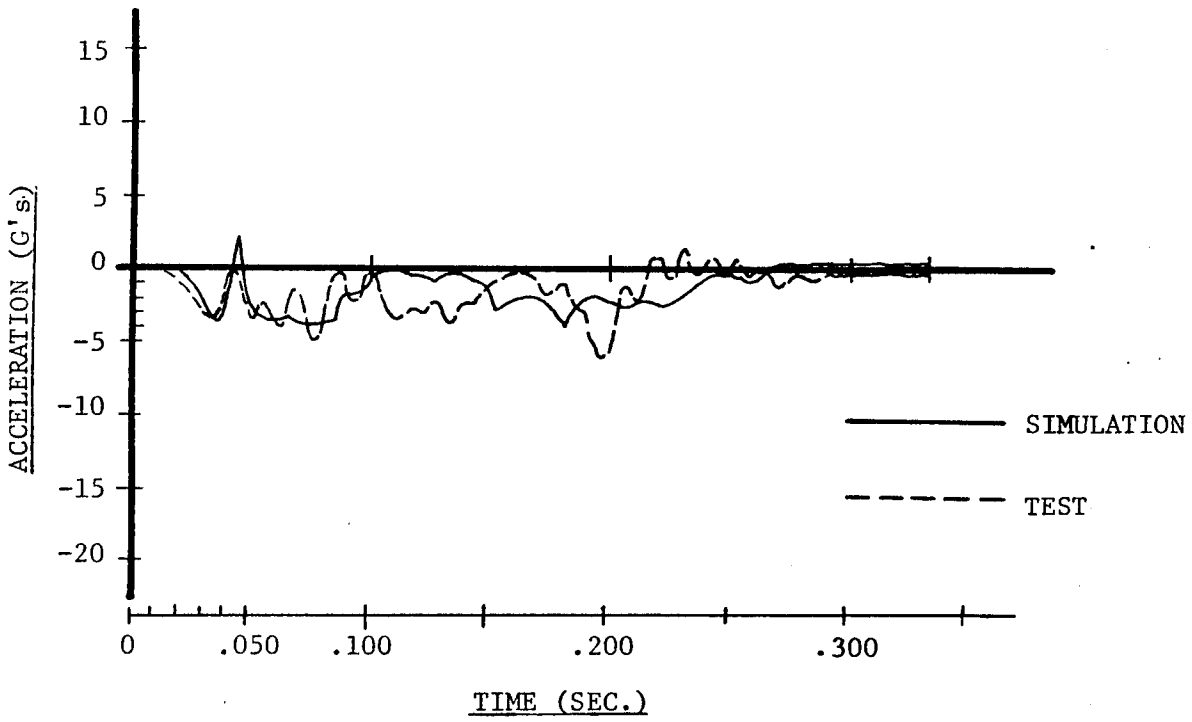

FIGURE 13.- LONGITUDINAL ACCELERATION ON IMPACT SIDE OF 4000 LB. VEHICLE IMPACTING CONCRETE MEDIAN BARRIER AT 63 MPH AT 25 DEGREES.

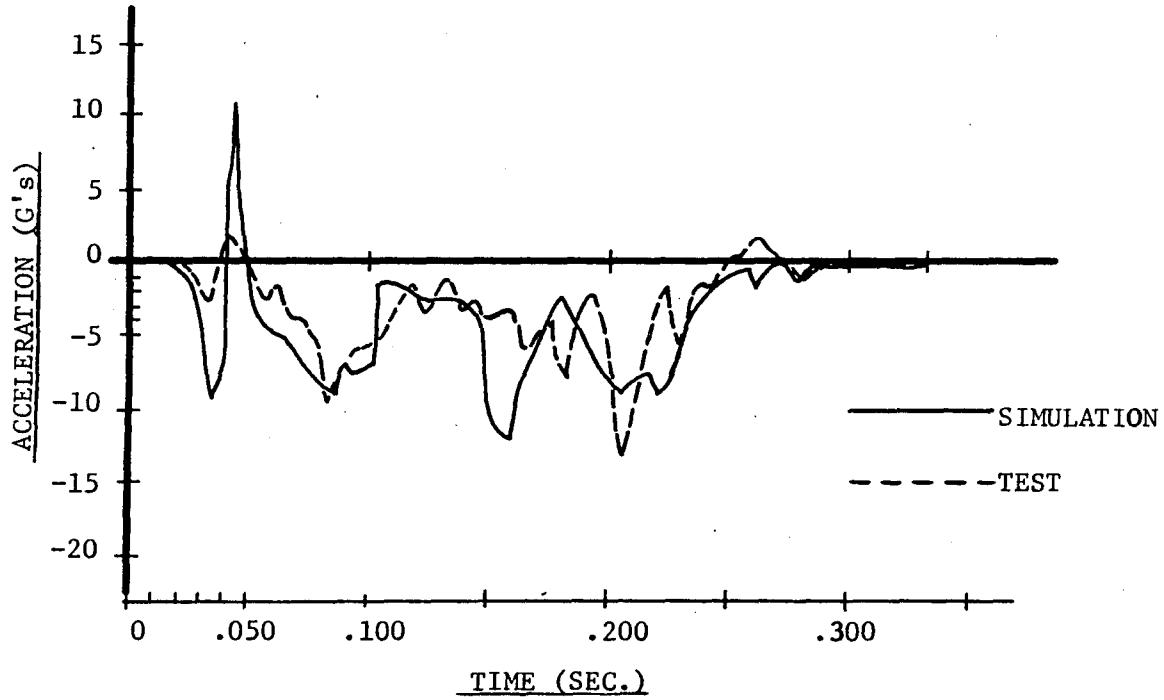

FIGURE 14. - LATERAL ACCELERATION ON FREE SIDE OF 4000 LB. VEHICLE IMPACTING CONCRETE MEDIAN BARRIER AT 63 MPH AT 25 DEGREES.

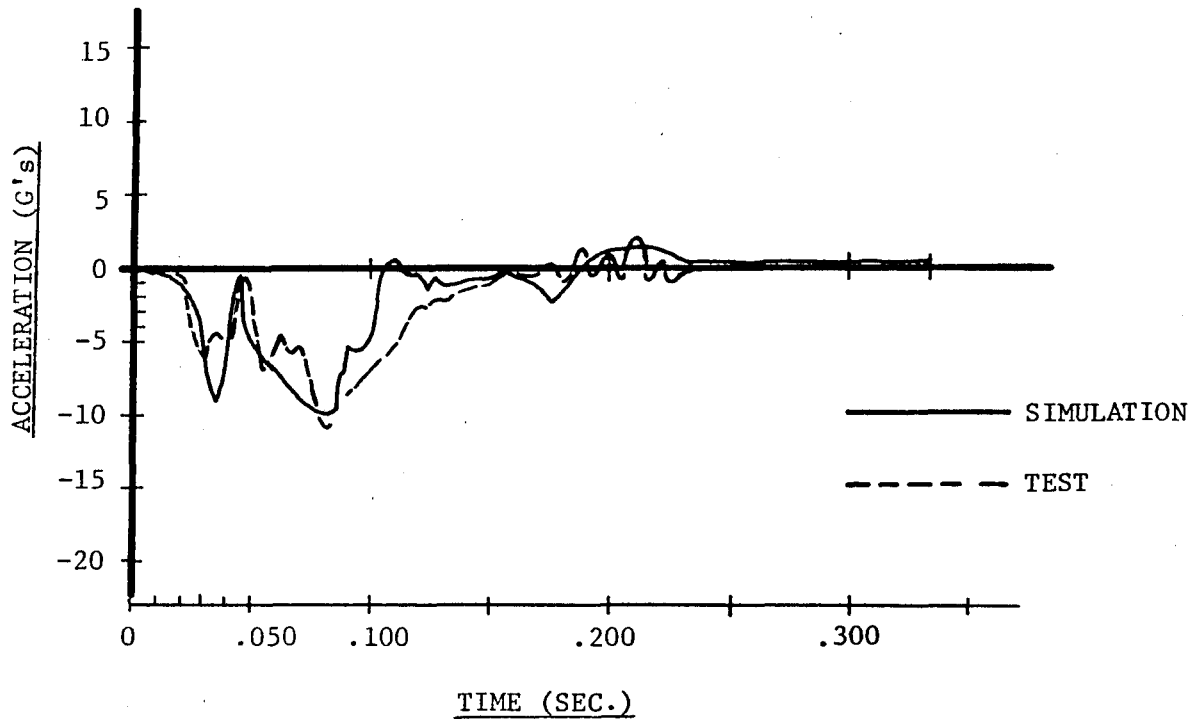

FIGURE 15.- LONGITUDINAL ACCELERATION ON FREE SIDE OF 4000 LB. VEHICLE IMPACTING CONCRETE MEDIAN BARRIER AT 63 MPH AT 25 DEGREES.

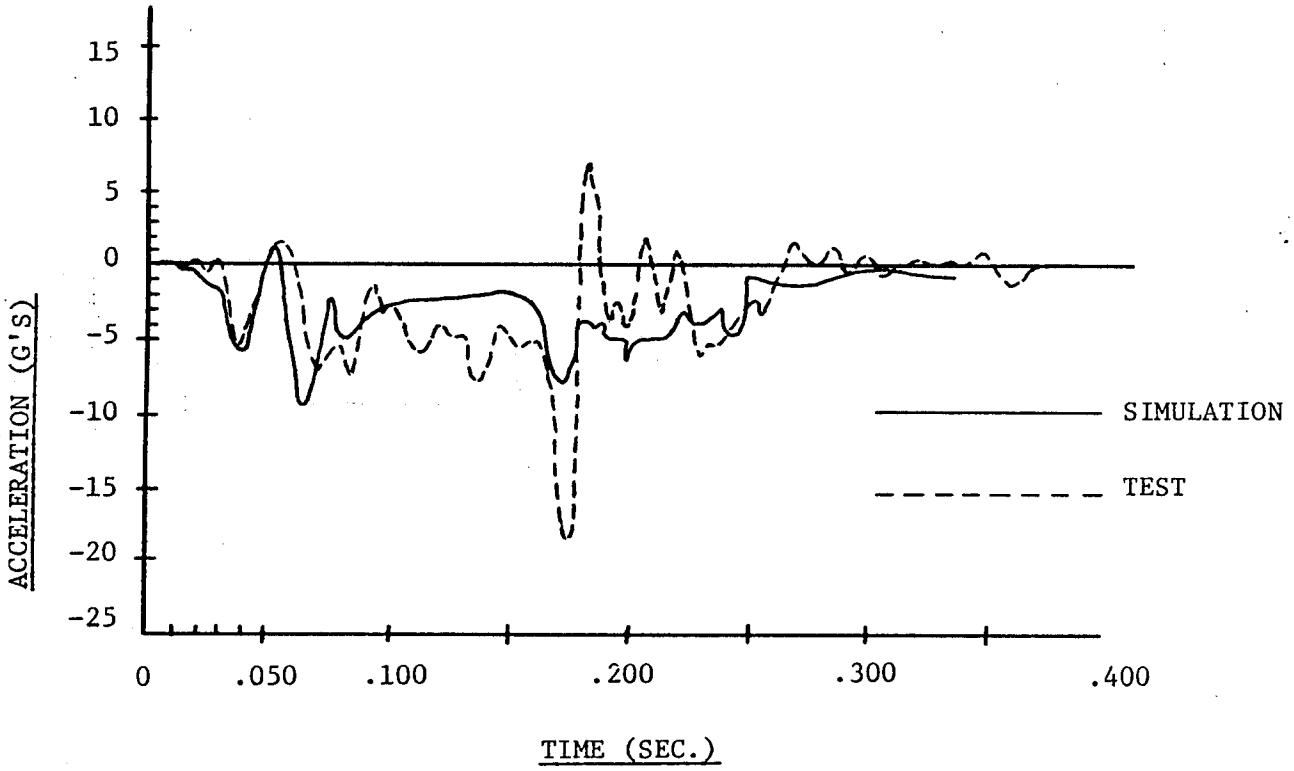

FIGURE 16- LATERAL ACCELERATION ON IMPACT SIDE OF 4210 LB. VEHICLE IMPACTING CONCRETE MEDIAN BARRIER AT 59.6 MPH AT 15 DEGREES.

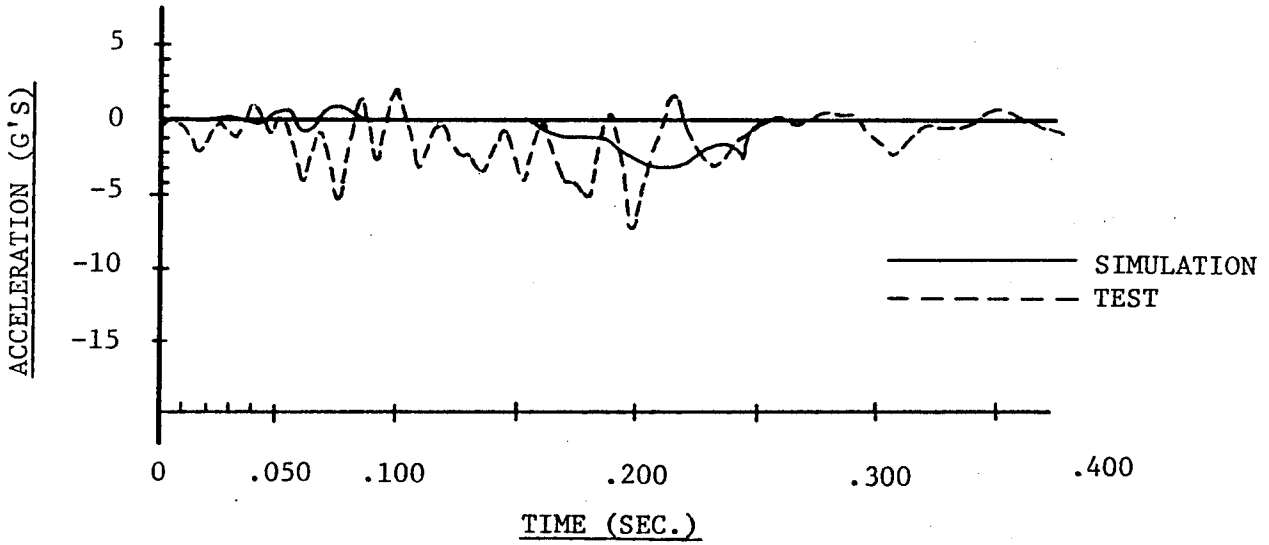

FIGURE 17 - LONGITUDINAL ACCELERATION ON IMPACT SIDE OF 4210 LB. VEHICLE IMPACTING CONCRETE MEDIAN BARRIER AT 59.6 MPH AT 15 DEGREES.

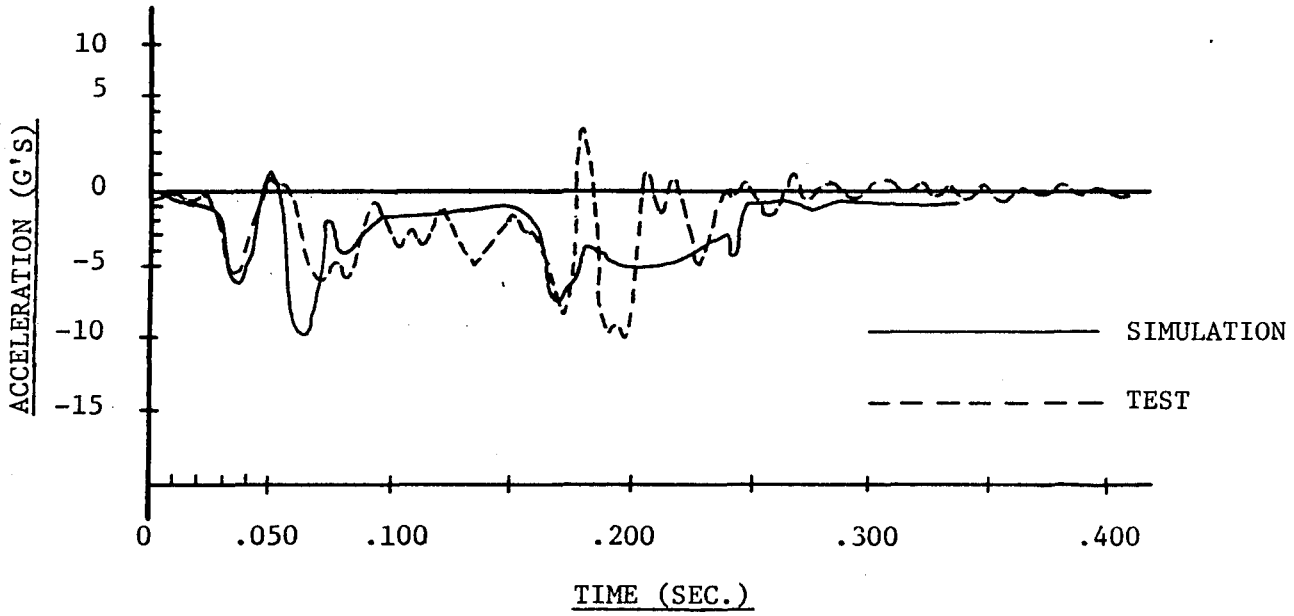

FIGURE 18 - LATERAL ACCELERATION ON FREE SIDE OF 4210 LB. VEHICLE IMPACTING CONCRETE MEDIAN BARRIER AT 59.6 MPH AT 15 DEGREES.

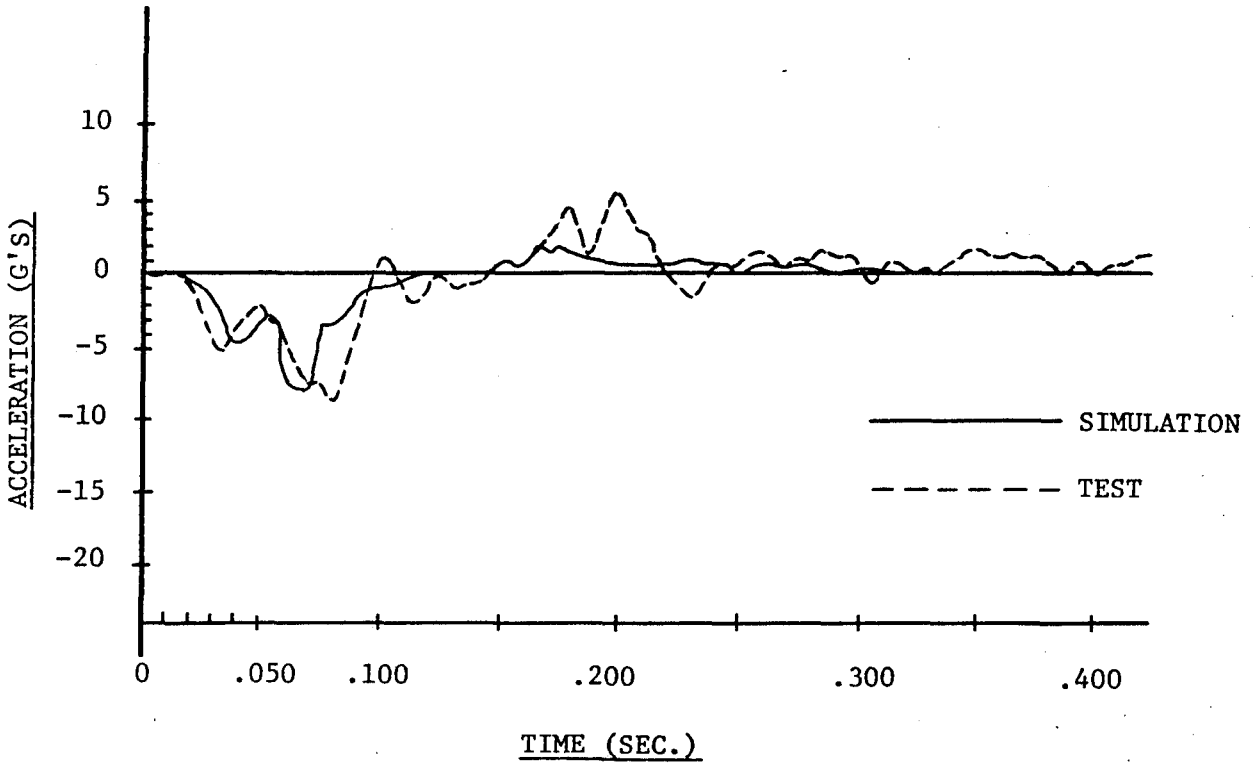

FIGURE 19 - LONGITUDINAL ACCELERATION ON FREE SIDE OF 4210 LB. VEHICLE IMPACTING CONCRETE MEDIAN BARRIER AT 59.6 MPH AT 15 DEGREES.

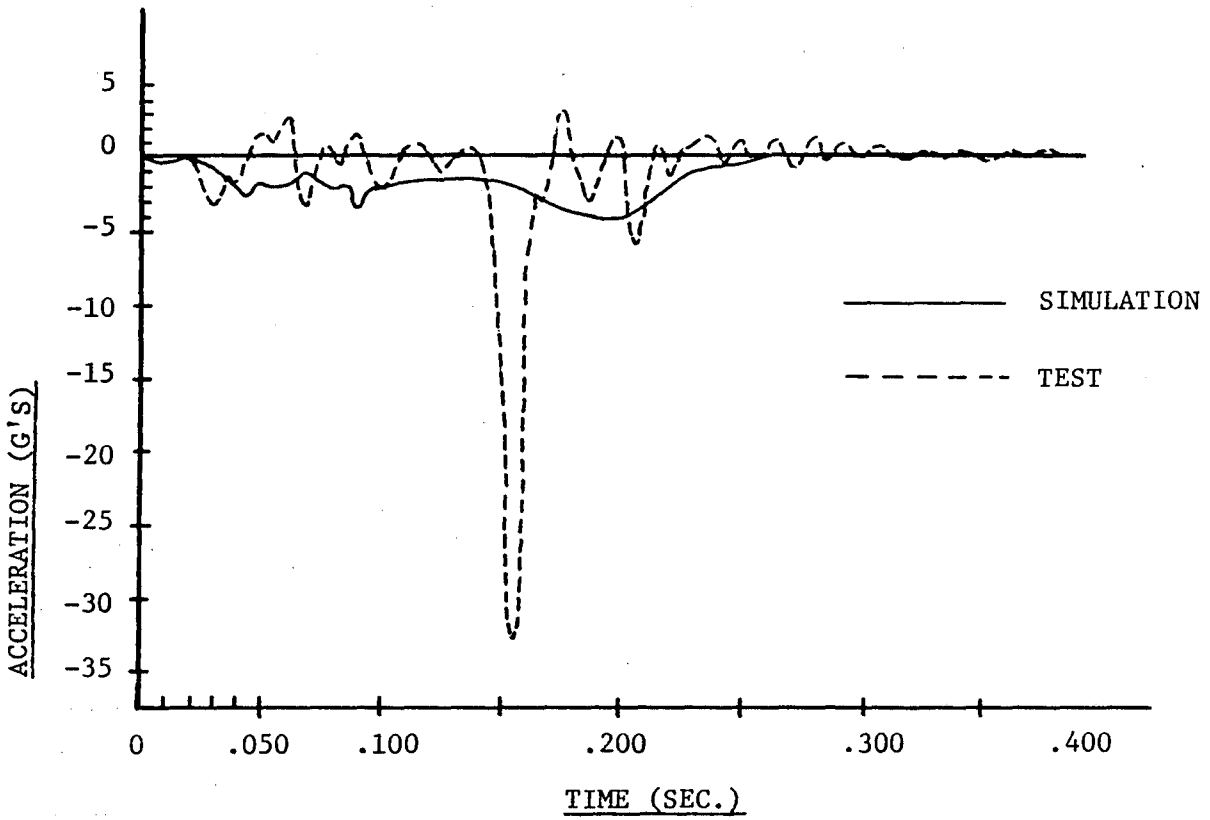

FIGURE 20 - LATERAL ACCELERATION ON IMPACT SIDE OF 4210 LB. VEHICLE IMPACTING CONCRETE MEDIAN BARRIER AT 61.9 MPH AT 7 DEGREES.

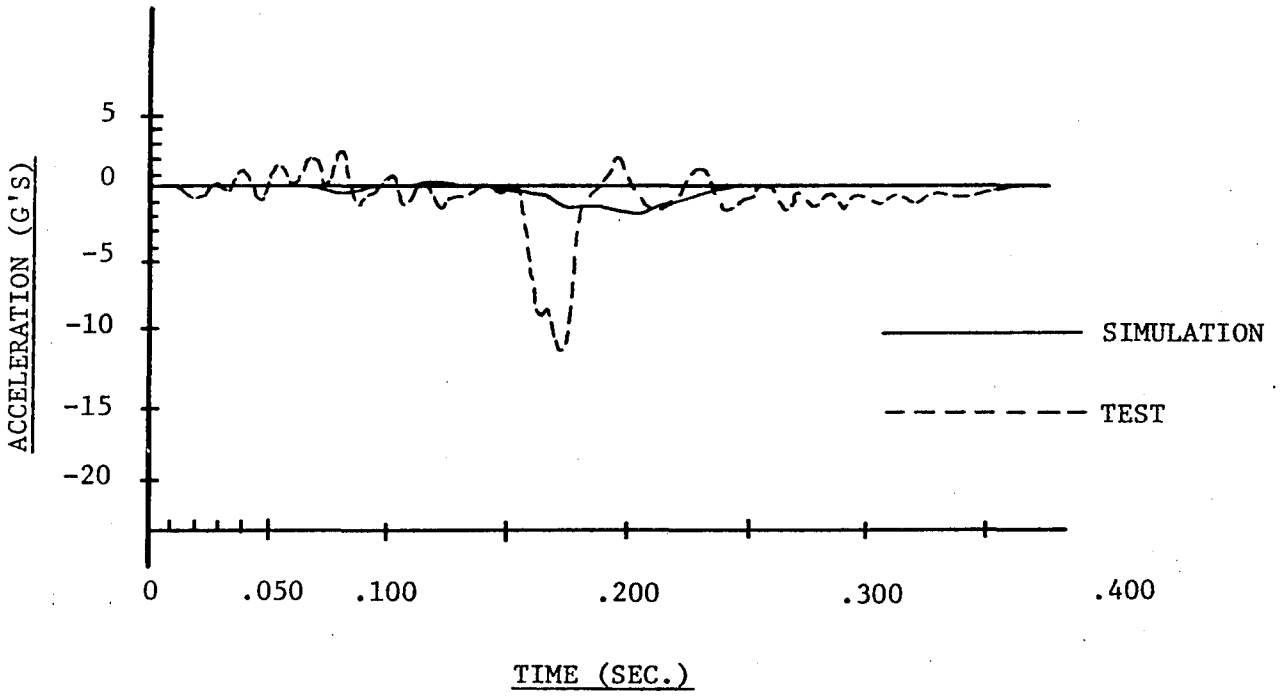

FIGURE 21 - LONGITUDINAL ACCELERATION ON IMPACT SIDE OF 4210 LB. VEHICLE IMPACTING CONCRETE MEDIAN BARRIER AT 61.9 MPH AT 7 DEGREES.

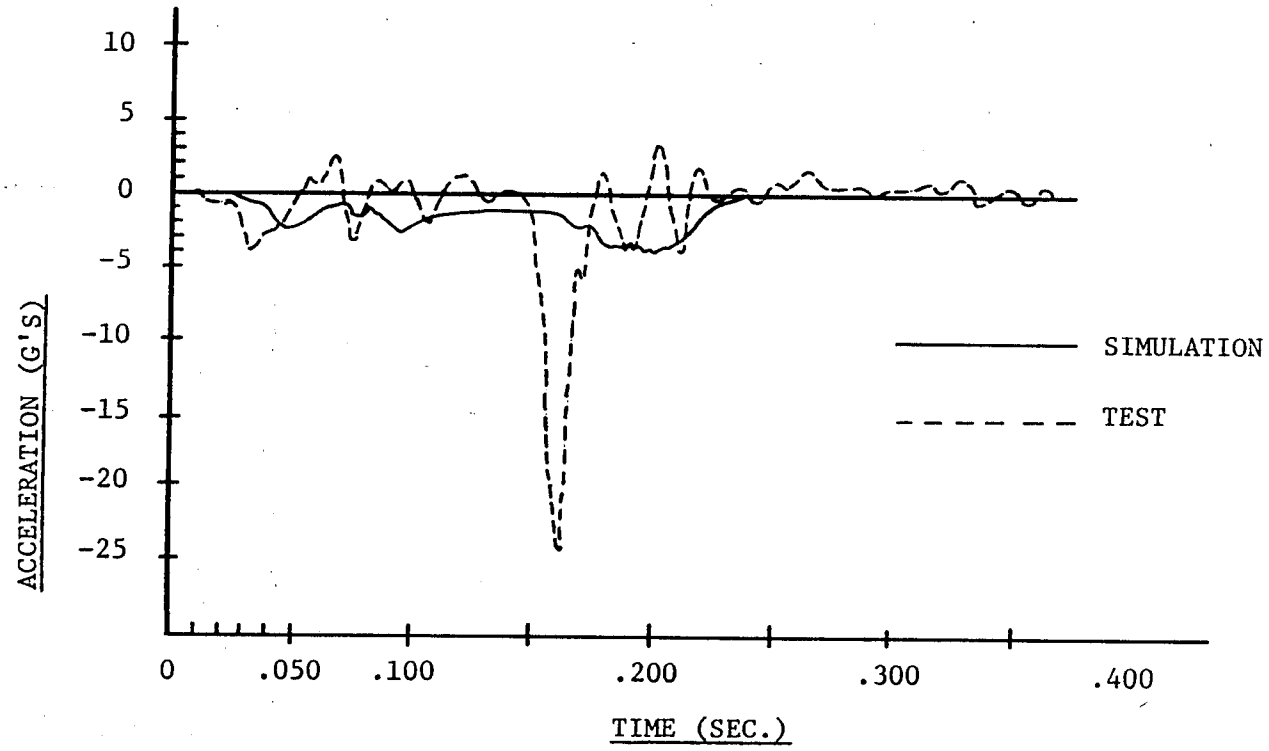

FIGURE 22 - LATERAL ACCELERATION ON FREE SIDE OF 4210 LB. VEHICLE IMPACTING CONCRETE MEDIAN BARRIER AT 61.9 MPH AT 7 DEGREES.

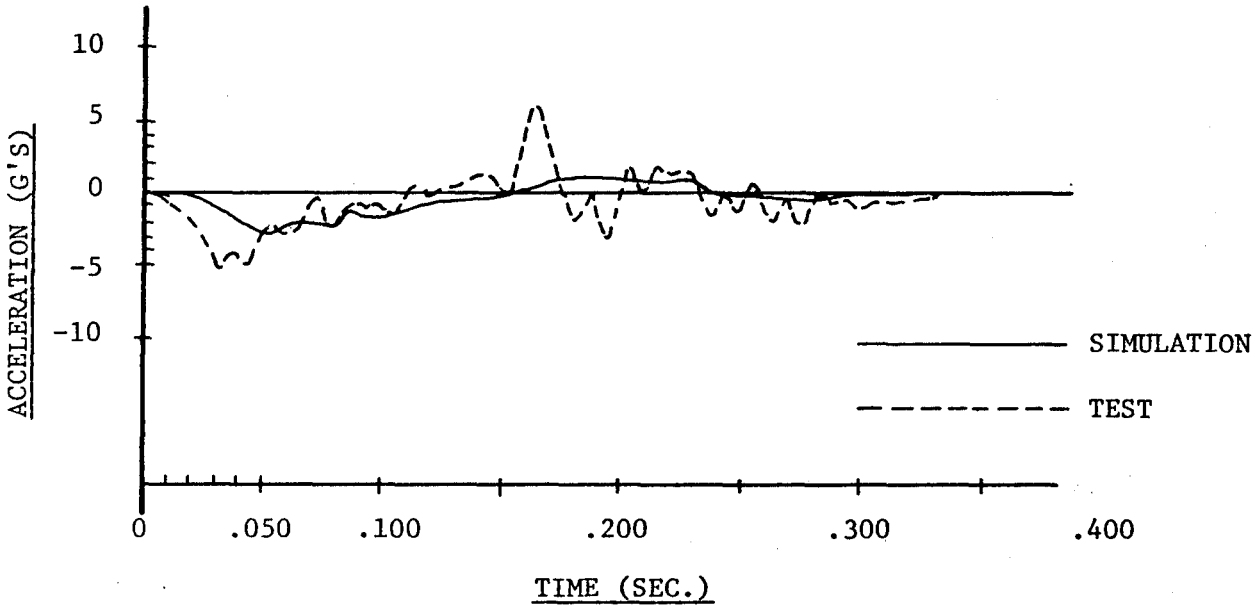

FIGURE 23 - LONGITUDINAL ACCELERATION ON FREE SIDE OF 4210 LB. VEHICLE IMPACTING CONCRETE MEDIAN BARRIER AT 61.9 MPH AT 7 DEGREES.

would not be felt by an occupant. Correspondingly, the simulated accelerometers respond only to those actions which cause vehicle redirection or rigid body motion since the simulation is devoid of structural vibrations except those stemming from the wheels and suspension systems.

2. In the actual case the effect of a force applied to the vehicle structure is diminished or damped before reaching an accelerometer located some distance away from the point of application. In some cases if the distance is large enough and the force is of short duration, the effect may be damped out completely and hence, undetected by the accelerometer. However, in the simulated case all forces applied to the vehicle structure are transferred to the center of gravity of the rigid body as an equivalent force-couple system such that all simulated accelerometers respond instantaneously regardless of their location on the structure.

The simulated accelerometer traces in Figures 12 and 14 exhibit an oscillation of $\pm$ 11 G's between 30 and 50 milliseconds which was not recorded by the test accelerometers. This is caused by the front wheel violently engaging the suspension bumper stops as it first hits the barrier at the large impact angle of 25 degrees. The same probably occurred in the test, but since the accelerometers were located about 6.5 ft behind the front wheel (just ahead of the rear wheel mounted to the frame member), the effects of these short duration forces were largely

damped out before reaching the accelerometers.

The test accelerometer traces in Figures 12, 16 and 18 reveal oscillations between 175 and 200 milliseconds which were not predicted by the simulation. These represent structural vibrations of the frame member, to which the accelerometers were mounted (just ahead of the rear wheel), induced by oscillations of the rear axle assembly when the rear wheel encountered the barrier. All of the differences in accelerations explained thus far were vibrational in nature and produced negligible net changes in velocity and hence, did not contribute to vehicle redirection. This is upheld by the fact that the comparisons of vehicle position are excellent (Figures 2 through 7).

The huge spike appearing in Figures 20 through 23 has 2 possible explanations. First, it is highly probable that this spike is also the result of a structural vibration caused by the rear wheel impacting the barrier. The vibration could have been critically damped explaining the existence of only 1 spike. Futhermore, the reason that higher G levels were recorded for this test, although it was less severe (only slight sheet metal damage), could be a result of the accelerometers being more directly aligned with the blow because of the small pitch and roll motions of the vehicle. If this explanation is accepted, the spike can be disregarded as not contributing to redirection of the vehicle, and the accelerometer comparison can be considered good.

However, as a second explanation, it is conceivable that initial tire contact caused the vehicle to rotate (yaw) parallel to the barrier

without appreciably changing the vehicle's velocity vector (magnitude nor direction). The vehicle would then have impacted the barrier in this position, causing an abrupt change in lateral velocity. In fact, for 60 mph at 7 degrees, the component of velocity normal to the barrier is 10.7 ft per second which corresponds to the area under the spike in question. This comparison is justifiable in this case since the car was parallel to the barrier when the spike occurred. If this explanation is accepted, the question remains as to whether this is a reproducible phenomenon or an abnormality. Until this question is answered, the HVOSM acceleromater results cannot be discounted, especially since good accelerometer comparisons were achieved for the 2 higher angles of impact, and good vehicle position comparisons were attained for all 3 tests.

Considering all facets of the comparison, it can be concluded that the HVOSM (with added structural hard points) provides a good simulation of an automobile impacting a rigid barrier of the Texas CMB type. Hence, it follows that the results of the parameter study (Chapter III) can be treated with added confidence.

III. PARAMETER STUDY

General

The modified version of the HVOSM computer program (including hard points, as described in Appendix B) was used to study the dynamic behavior of an automobile impacting the Texas CMB. The objective of the parametric study was to determine the performance characteristics of the CMB for a range of vehicle encroachment conditions. Factors used to measure barrier performance consisted of the vehicle's exit angle, maximum pitch and roll angle, and a severity index to quantify the event severity. The index is an interaction formula involving vehicle acceleration components and tolerable vehicle accelerations. It is discussed in Appendix D.

Nine different automobile impacts with the CMB were simulated. The impact speeds were 50, 70, and 80 mph and for each speed there were three impact angles; 5, 10, and 15 degrees. The simulated automobile had the properties of a 1963 Ford Galaxie weighing 4,780 pounds. Also included in this phase of the study were the three impacts simulated in the validation study (Chapter II), consisting of impact angles of 7, 15, and 25 degrees at an impact speed of approximately 60 mph. These twelve different impact conditions are representative of the majority of accidents involving traffic barriers. The results of the twelve runs are presented in Table 1.

All impact data for the computer runs, including vehicle and barrier information, are given in Volume II of this report. Some of the significant parameters were as follows:

TABLE 1

RESULTS OF CMB BARRIER SIMULATIONS

RUN NO.	AUTO WEIGHT	IMPACT CONDITIONS		AUTOMOBILE KINEMATICS				AVERAGE ACCELERATIONS DURING PRIMARY IMPACT			
	(LBS)	SPEED (MPH)	ANGLE, θ_1(DEG)	MAX. ROLL (DEG)	MAX. PITCH (DEG)	FRONT TIRE CLIMB (IN)	EXIT ANGLE** θ_2 (DEG)	G_{LONG}	G_{LAT}	G_{VERT}	S.I.***
1	4780	50.0	5.0	1.3	0.9	4.6	1.1	0.49	1.61	0.12	0.33
2	4780	70.0	5.0	2.2	1.5	6.5	0.3	0.72	2.53	0.43	0.52
3	4780	80.0	5.0	3.3	1.8	7.1	0.1	0.21	2.90	0.54	0.58
4	4780	50.0	10.0	4.2	3.2	8.6	2.5	1.13	2.99	0.94	0.64
5	4780	70.0	10.0	19.5*	5.0	11.2	1.2	0.16	5.06	2.03	1.07
6	4780	80.0	10.0	34.6*	5.8	12.6	1.2	1.92	6.42	2.61	1.38
7	4780	50.0	15.0	15.0*	6.5	11.9	3.6	0.47	4.29	1.38	0.91
8	4780	70.0	15.0	RO	6.6	NA		2.81	6.44	3.16	1.45
9	4780	80.0	15.0	RO	6.1	NA		3.24	7.49	3.29	1.66
10	4210	61.9	7.0	4.7	2.3	7.4	2.2	1.07	3.21	0.64	0.67
11	4210	59.6	15.0	21.0*	8.2	13.2	5.5	2.78	6.86	2.92	1.48
12	4000	63.0	25.0	37.0	8.6	NA	5.1	6.47	11.23	4.38	2.54

*Estimated roll obtained by energy expression using initial conditions from computer simulation at the time it was terminated. (See Appendix E)
**When vehicle loses contact with barrier.
***From Equation D1.
RO=Rollover
NA=Not available

Hardpoint Stiffness	= 2500 LB/IN
Sheet Metal Crushing Coefficient	= 2 LB/IN^3
Auto-Barrier Coefficient of Friction	= 0.3
Tire-Curb Coefficient of Friction	= 0.50

In some instances, the roll angle of the vehicle was still increasing at the termination of the computer run. Rather than re-run those cases (which would have been uneconomical) a formula was developed to estimate the roll angle beyond the termination point. This relationship was used to determine the maximum roll angle. Its derivation is given in Appendix E.

Barrier Performance

Model simulation indicates that the vehicle will roll over during a collision with a CMB at impact speeds of 70 and 80 mph and an impact angle of 15 degrees. The roll angle reported in Table 1 is the maximum roll angle of the automobile and may or may not occur when the automobile is in contact with the barrier.

As shown in Table 1, the maximum pitch angle of the automobile appears more sensitive to impact angle than to impact speed. In any event, the pitch angle remains small for any angle of impact and appears to be insignificant when considering the motion of the automobile.

Height of climb of the front tire on the face of the CMB is given in Table 1. During a 5 degree collision, the front tire of the automobile climbs roughly 5 to 7 inches on the lower inclined CMB surface; and, during

a 10 degree collision the tire climbs roughly 9 to 12 inches on the lower surface. As indicated, the climb height was not available in some cases becuase tire-rigid barrier interaction is not accounted for in HVOSM (see discussion in Chapter II). However, based on an analysis of the output, it is doubtful that the tire climb would have exceeded the height of the barrier in those cases.

A desirable characteristic of a traffic barrier is that a colliding automobile be redirected at a shallow exit angle in order to minimize the danger to traffic. The exit angles shown in Table 1 were determined at the time the vehicle lost contact with the barrier. The exit angle appears to be more sensitive to impact angle than to impact speed. In all cases, however, the exit angles were shallow.

Another criterion used to determine barrier performance was the relative severity of the impact as measured by automobile accelerations. A severity index, which quantifies the severity, was computed and listed in Table 1 for each of the twelve runs studied. A discussion of the index is given in Appendix D.

Figure 24 shows the severity index versus impact angle for four different impact speeds. The apparent inconsistency of the 60 mph case is attributable to the differences in vehicle weight and dimensions. For vehicle speeds of 50, 70, and 80 mph the vehicle weighed 4,780 pounds, whereas, in the 60 mph case the vehicle weighed 4,210 pounds. The hard-point stiffness, sheet metal crushing coefficient, auto-barrier coefficient of friction, and tire-curb coefficient of friction were the same for all four speeds. The results therefore suggest that the severity of a lighter

FIGURE 24. - SEVERITY INDEX OF CMB AS RELATED TO VEHICLE ENCROACHMENT CONDITIONS

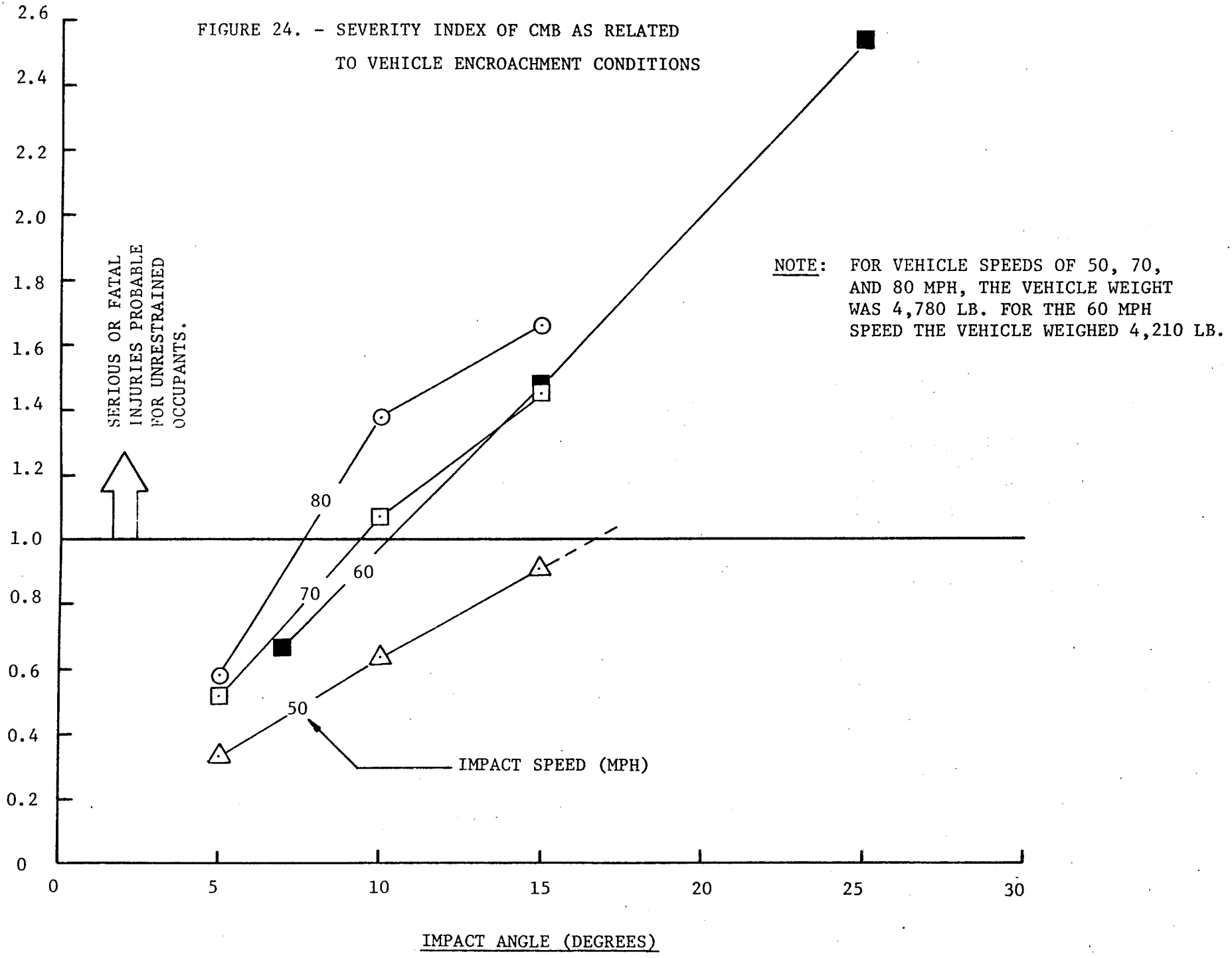

NOTE: FOR VEHICLE SPEEDS OF 50, 70, AND 80 MPH, THE VEHICLE WEIGHT WAS 4,780 LB. FOR THE 60 MPH SPEED THE VEHICLE WEIGHED 4,210 LB.

vehicle impacting the barrier is higher than for a heavier vehicle, all other factors being the same.

Figure 25 shows impact speed versus impact angle for a severity index of one (1.0). The four points on the curve in Figure 25 were obtained from the intersection of the SI = 1.0 line with the four respective speed curves of Figure 24. The data as presented in Figure 25 may be useful in selecting roadway locations where the CMB can be safely used. For a given roadway, an upper limit on impact angle can be estimated as a function of the roadway's design speed and surface conditions and the distance from the roadway to the barrier.(6) If the combination of design (or impact) speed and impact angle falls above the curve it may be advisable to select a more flexible barrier.

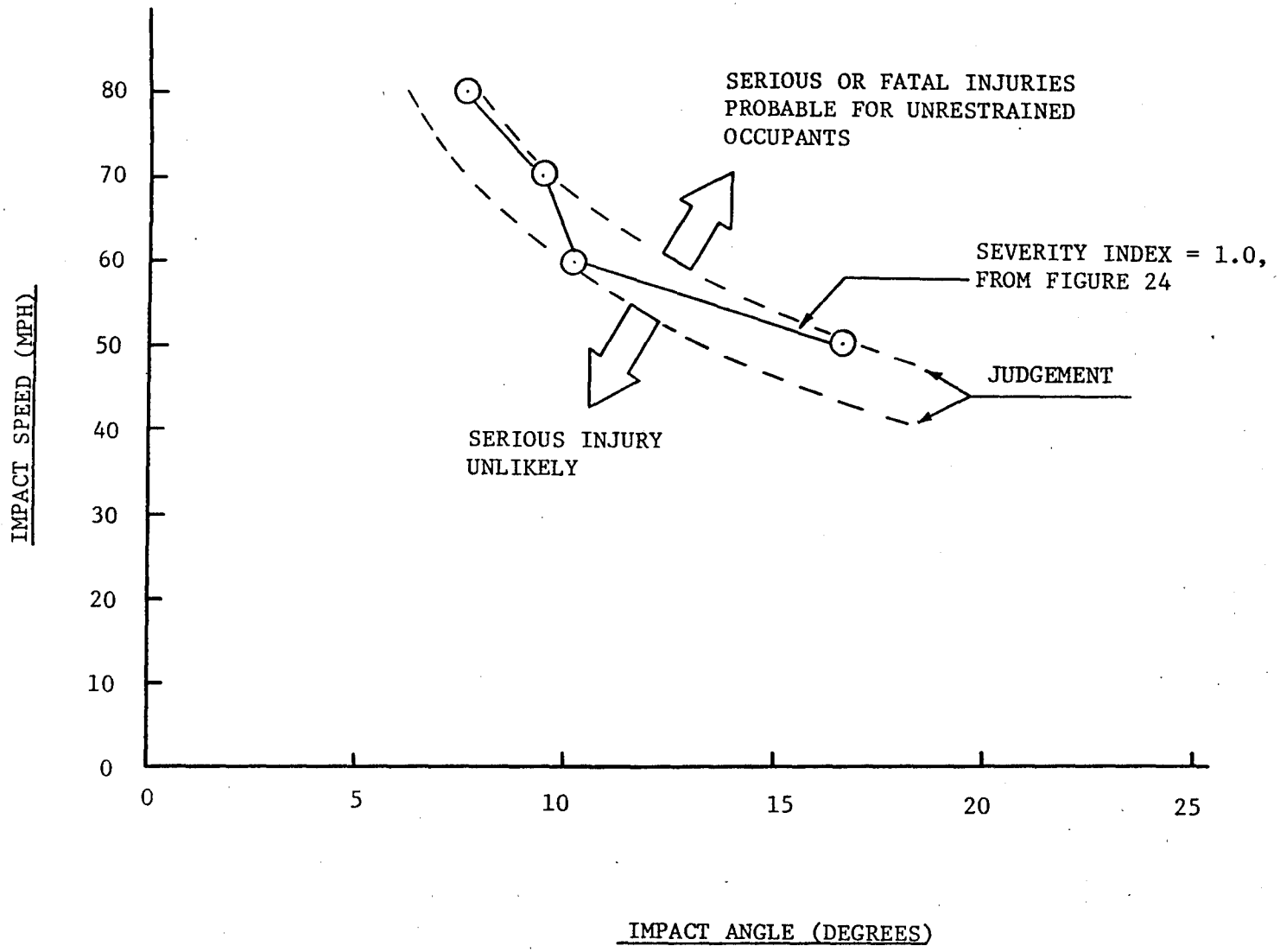

FIGURE 25. - RELATION BETWEEN ENCROACHMENT CONDITIONS AT A SEVERITY INDEX NEAR UNITY FOR CMB

IV. CONCLUSIONS

1. The impact subroutines of HVOSM were modified by TTI to account for the effects of *hardpoint* contacts (frame members, motor block, etc.) which occur when large vehicle deformations occur.
2. The modified HVOSM computer program (with hardpoints) can accurately predict automobile accelerations, motions, and external forces due to an impact with the Texas Concrete Median Barrier. This conclusion is based on a good correlation that was obtained between full-scale test results and simulations by HVOSM.
3. As a result of a parametric study with HVOSM, the following conclusions are made with regard to the Texas Concrete Median Barrier's performance:
   (a) For impact speeds of 70 mph and greater in conjunction with impact angles of 15 degrees and greater, automobile rollover can be expected. This is a redundant finding in one respect since the severity indices indicate that serious or fatal injuries can be expected for these encroachment conditions. However, it is indeed an important consideration in view of the hazard that a rollover creates for other motorists.
   (b) For impact speeds of 80 mph and less at impact angles of 15 degrees and less there was no tendency for the automobile to vault or climb over the barrier.
   (c) In each of the ten impact conditions studied, where rollover did not occur, the automobile's exit angle was shallow after impact with the barrier (less than 6 degrees).
   (d) A graphical presentation of the impact angles and speeds for which

the barrier can redirect an automobile without serious injuries to the occupants is given in Figure 25. This graph will aid the highway designer in deciding whether to install a CMB or a more flexible barrier. For instance, if the design speed is 70 mph, the width of roadway should be sufficiently narrow that an errant vehicle would impact the CMB at no greater than 10 degrees. (An estimate of maximum roadway width for a desired impact angle can be made using an equation suggested by Deleys (6)).

V. RECOMMENDATIONS

In view of the research findings the authors recommend the following:

1. further application of HVOSM in studying alternate shapes for the CMB in an effort to find one which will restrict the threat of rollover to much higher speeds and impact angles;
2. refinement of the severity index by taking a closer look at the relationship between accelerations experienced by the vehicle and the corresponding injury to the occupant. The current state-of-the-art requires one to assume that occupant accelerations equal those encountered by the vehicle. The validity of this assumption is questionable (especially for the unrestrained occupant) and as such it reduces the confidence level of the computed severity index. TTI is currently extending the development of a vehicle-victim model (on a separate study) that was initiated in Project 140 (7). This model will provide a means to determine the relationship between vehicle and occupnat accelerations. This would enable a refinement of Figure 25 making it more objective and hopefully broadening its design application. For example, Figure 25 would require a safe impact angle of 7.5° maximum at 70 mph which is highly restrictive; and
3. parameter studies aimed at the performance of the CMB for a range of vehicle sizes, weights, and suspension properties.

APPENDIX A

A DESCRIPTION OF THE HIGHWAY-VEHICLE-OBJECT SIMULATION MODEL

APPENDIX A

A Description of the Highway-Vehicle-Object Simulation Model

To facilitate in the evaluation and design of a roadway and its environment, it is important to understand what effects that various roadway geometric features have on the dynamic behavior of an automobile and its occupnats.

The mathematical model described herein is known as The Highway-Vehicle-Object Simulation Model (HVOSM). In general, this model can be utilized to investigate various problems associated with the roadway environment, such as highway traffic barrier collisions, rapid lane change maneuvers, handling response on horizontal curves, drainage ditch cross sections, and others.

The HVOSM was developed by Cornell Aeronautical Laboratory (CAL) (1, 2) and later modified for specific problem studies by the Texas Transportation Institute (TTI) (8). A conceptual idealization of the model is shown in Figure A1. The model is idealized as four rigid masses, which include: (a) the sprung mass (M_S) of the body supported by the springs, (b) the unsprung masses (M_1 and M_2) of the left and right independent suspension system of the front wheels, and (c) the unsprung mass (M_3) representing the rear axle assembly.

The eleven degrees of freedom of the model include translation of the automobile in three directions measured relative to some fixed coordinate axes system; rotation about the three coordinate of the automobile; independent displacement of each front wheel suspension

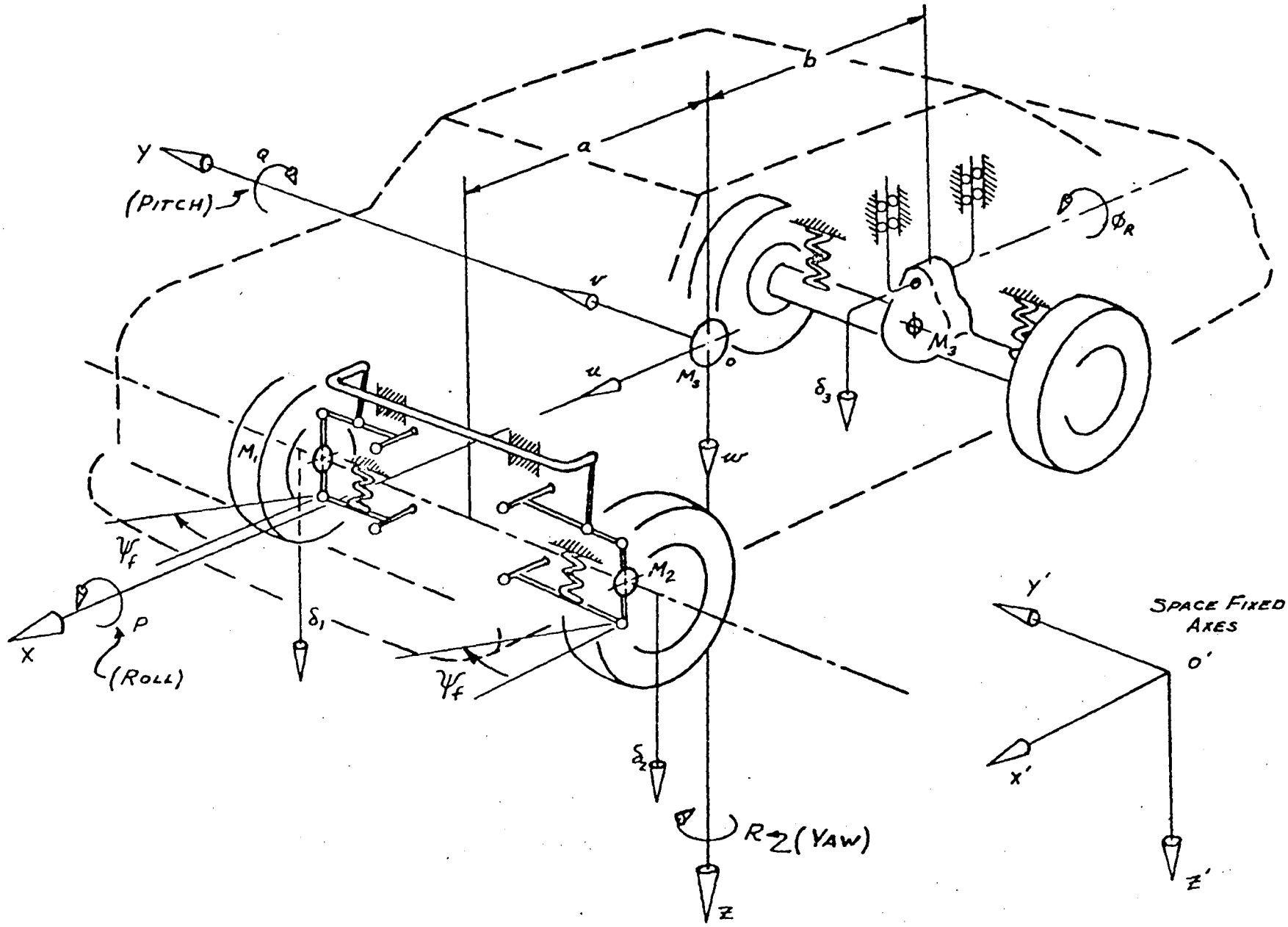

FIGURE A1. IDEALIZATION OF AUTOMOBILE (1,2)

system; suspension displacement and rotation of the rear axle assembly; and steer of the front wheels. If interested, the reader is referred to the references quoted earlier for a more in depth discussion of the mathematical model.

APPENDIX B

THE ADDITION OF STRUCTURAL HARDPOINTS TO THE ORIGINAL HVOSM

APPENDIX B

The Addition of Structural Hard Points to the Original HVOSM

During TTI's initial attempts at simulating automobile collisions with a rigid type barrier, it became obvious that for large angles of attack (characterized by heavy sheet metal crushing), the HVOSM needed modification to account for the high impact forces resulting from stiff automobile structural components (hard points) slamming into the barrier.

According to McHenry et al.'s description of their mathematical model (2, pp. 126-129), the collision properites of the vehicle structure stem from an idealized layer of isotropic, homogenous, plastic material which surrounds the vehicle. They never intended this representation for anything more than simulating sheet metal crush of moderate penetration (i.e., 12 to 18 inches). In fact, McHenry and Deleys were the first to realize the need to account for structural hard points as they had formulated the problem (including preliminary computer programming) prior to TTI's request for assistance in the matter. They generously provided TTI with copies of their work which

proved to be a momentous contribution toward modifying the HVOSM and ultimately led to a successful simulation of an automobile impacting the Texas CMB.

Conceptually the idea of hard points was quite simple as it merely required defining (as input to HVOSM) the location of the desired points on the vehicle and the stiffness of each. The difficulty arose in trying to weave that concept into the existing fabric of sophisticated logic comprising the sprung-mass impact subroutines of the HVOSM. This is where CAL's assistance proved invaluable.

The new input variables required to define the hardpoints are as follows:

XSTIO (J) YSTIO (J) ZSTIO (J)	-	Coordinates of original position of hard point no. J in vehicle-fixed coordinate system
AKST (J)	-	Stiffness (lbs./in.) of hard point no. J, assumed to be omnidirectional

A listing of subroutine "SFORCE" is provided in this appendix. It shows the computation and use of the following quantities:

YSTIPO (J)	-	the Y position of undeformed hardpoint no. J in space-fixed coordinates
XSTIP (J) YSTIP (J) ZSTIP (J)	-	the coordinates of the present position (deformed state) of hard point no. J in space-fixed coordinates
FNSTI (J)	-	force (lbs.) on deformed hard point no. J

SFNST	-	the sum of forces on all hard points for an assumed barrier deflection during iteration for equilibrium
FNX1	-	force due to sheet metal crushing for an assumed barrier detection
FNX	=	FNX1 + SFNST, i.e., total force derived from barrier impact for an assumed barrier deflection
FN	-	force due to sheet metal crushing the barrier in its equilibrium position
FN1	=	FN + SFNST, i.e., total force derived from barrier contact for barrier in equilibrium position
XSTI (J) YSTI (J) ZSTI (J)	-	coordinates of hard point no. J (deformed state) in vehicle-fixed coordinates

A listing of subroutine "RESFRC" is also included in this appendix to show the manner in which the forces derived from sheet metal crushing and various hard point impacts are resolved into forces and couples at the vehicle's center of gravity.

```
COMPILER OPTIONS - NAME=  MAIN,OPT=02,LINECNT=60,SOURCE,EBCDIC,NOLIST,NODECK,LOAD,MAP,'
      C     SINGLE VEHICLE ACCIDENT SIMULATION - SUBROUTINE SFORCE                  SFRC   1
            SUBROUTINE SFORCE                                                       SFRC   2
            COMMON/INPT/PHIO,THETAO,PSIO,PO,QO,RO,XCOP,YCOP,ZCOP,UO,VO,WO,A,B,      SFRC   3
           1            DEL1O,DEL2O,DEL3O,PHIRO,DEL1OD,DEL2OD,DEL3OD,PHIROD,TF      SFRC   4
           2           ,TR,ZF,ZR,RHO,RW,AKT,SIGT,XLAMT,A1,A2,A3,AKRS,AMU,XMUR,      SFRC   5
           3            XMS,XMUF,XIX,XIY,XIZ,XIXZ,CF,AKF,XLAMF,OMEGF,CFP,EPSF,      SFRC   6
           4            RF,CP,AKR,XLAMR,OMEGR,CRP,EPSR,RR,TS,THMAX,DTCOMP,TO,       SFRC   7
           5            T1,DTCMP1,DTPRNT,MODE,EBAR,EM,AAA,HMAX,HMIN,BET,G,          SFRC   8
           6            HED(36),DADE(3),XIR,X1,Y1,Z1,X2,Y2,Z2,PHIC(50),DELB,        SFRC   9
           7            DELF,DDEL,NDEL,PSIF(50),TQF(50),TQR(50),TB,TE,TINCR,        SFRC  10
           8            XBDRY(10),YBDRY(10),ZGP(21,21),THG(21,21),PHIG(21,21),      SFRC  11
           9            XB,XE,XINCR,NX,YB,YE,YINCR,NY,NBX,NBY,UVWMIN,PQRMIN         SFRC  12
            COMMON/INPT1/YC1P,YC2P,ZC2P,DELTC,PHIC1,PHIC2,AMUC,FJP(35),XIPS,        SFRC  13
           1             CPSP,OMGPS,AKPS,EPSPS,XPS,RWHJB,RWHJE,DRWHJ,INDCRB,       SFRC  14
           2             PSIFIO,PSIFDO                                             SFRC  15
            COMMON /INTG/NEQ,T,DT,VAR(50),DER(50)                                   SFRC  16
            COMMON /DIMV/X1P,X2P,X3P,X4P,Y1P,Y2P,Y3P,Y4P,Z1P,Z2P,Z3P,Z4P,PHI1,      SFRC  17
           1             PHI2,PHI3,PHI4,PSI1,PSI2,PSI3,PSI4,CAYW(4),CBYW(4),       SFRC  18
           2             CGYW(4),ZPGI(4),THGI(4),PHGI(4),CPG(4),SPG(4),CTG(4),     SFRC  19
           3             STG(4),CAGZ(4),CBGZ(4),CGGZ(4),D1(4),D2(4),D3(4),         SFRC  20
           4             XLM1(4),XLM2(4),XLM3(4),AMTX(3,3),CMTX(3,4),XGPP(4),      SFRC  21
           5             YGPP(4),ZGPP(4),DMATX(10,11),DELTA(4),CAR(4),CBR(4),      SFRC  22
           6             CGR(4),FR(4),HI(4),FC(4),TI(4),AX(4),BX(4),CX(4),         SFRC  23
           7             CTXG(4),UG(4),STXG(4),AY(4),BY(4),CY(4),CPYG(4),          SFRC  24
           8             SPYG(4),VG(4),PSIIP(4),PHICI(4),CAC(4),CBC(4),CGC(4),     SFRC  25
           9             FCXU(4),FCYU(4),FCZU(4),FS(4),CAXW(4),CBXW(4),CGXW(4)     SFRC  26
            COMMON /DIMV/AS(4),BS(4),CS(4),CAS(4),CBS(4),CGS(4),BETP(4),            SFRC  27
           1             BETBR(4),FSXU(4),FSYU(4),FSZU(4),FRXU(4),FRYU(4),         SFRC  28
           2             FRZU(4),FXU(4),FYU(4),FZU(4),SI(4),F1FI(2),F1RI(2),       SFRC  29
           3             F2FI(2),F2RI(2),CAH(4),CBH(4),CGH(4)                      SFRC  30
            COMMON /COMP/SUMM,THETN,PHIN,PSIN,PI,RAD,GAM1,GAM2,GAM3,GAM4,GAM5,      SFRC  31
           1             GAM6,GAM7,GAM8,GAM9,THETT,PHIT,PSIT,A12,A23,ZRO,TRO2,     SFRC  32
           2             TFO2,TIZ,RHO2,RHOMUR,AMUF,BMUR,ZPR,TM4,RHMR2,A02APB,      SFRC  33
           3             BO2APB,RFTF,TSO2,RRTS,BROMUR,XMUFO2,AXMFO2,XMTFO4,        SFRC  34
           4             XIZR,RTR,RHMR2I,XIXP,XIZP,XIXZP,XIYZP,D1PD2,D1MD2,        SFRC  35
           5             ZRD3,ZRD3R,ZFD3R,ZFD12,TIZ2,TG61,DD1P2,DD1M2,RPR,PHRP     SFRC  36
           6            ,TANTP,SPHTP,CPHTP,SECTP,SFXS,SFYS,SFZS,SNPS,SNTS,         SFRC  37
           7             SNPSS,TPR,CAY,CBY,CGY,CAX,CBX,CGX,SFYU,SFXU,SFYUF,        SFRC  38
           8             SFYUR,SFZU,COSTH,SINTH,COSPS,SINPS,COSPH,SINPH,ANG1,      SFRC  39
           9             ANG2,CPHI,SPHI,CPSI,SPSI,P1,P7,P3,P4,P5,P6,TX,TY,TZ       SFRC  40
            COMMON /COMP/TRH,DISTX,DISTY,DISTD,DISTS,D21,ZETA4,ZETA4D,ZETA3,        SFRC  41
           1             ZETA3D,SFZ1,SNPU,SNTU,HCGH1,HCGH2,HCGH3,HCGH4,TERM1,      SFRC  42
           2             TERM2,SNPSU,SNPR,HCBH1,HCBH2,HCBH3,HCBH4,HCAH1,HCAH2,     SFRC  43
           3             HCAH3,HCAH4,UQ,WP,UR,QR,VP,PR,P2,Q2,R2,VR,WQ,PQ,PHIR2     SFRC  44
           4            ,PHIRD2,RPHRD,GCTH,GSTH,GCTSP,GCTCP,XXX,YYY,IX,IY,XX1,     SFRC  45
           5             XX2,YY1,YY2,THG1,THG2,PHG1,PHG2,ZZ1,ZZ2,LLL               SFRC  46
            COMMON /COMPN/ OMT2M1,FRSP(4),FRCP(4),OMEGT,ICBHIT,JCBHIT,              SFRC  47
           1               DPSINT,TANPC1,TANPC2,PHIC1R,PHIC2R,AMUCMP,PHI1D,       SFRC  48
           2               PHI2D,LCB1(4),LCB2(4),IHIT,AJMTX(3,3),BMTX(3,3),       SFRC  49
           3               SFRX(4),SFRY(4),SFRZ(4),T1PSI,T2PSI,XMU                SFRC  50
            COMMON/ADTNL/U1,U2,U3,U4,V1,V2,V3,V4,W1,W2,W3,W4,XTRA(300)              SFRC  51
            DIMENSION XP(4),YP(4),ZP(4),PHII(4),PSII(4),UI(4),VI(4),WI(4)         SFRC  52
            EQUIVALENCE (XP,X1P),(YP,Y1P),(ZP,Z1P),(PHII,PHI1),(PSII,PSI1),       SFRC  53
           1            (UI,U1),(VI,V1),(WI,W1)                                   SFRC  54
            EQUIVALENCE (U,VAR(1)),(V,VAR(2)),(W,VAR(3)),(P,VAR(4)),(Q,VAR(5))    SFRC  55
           1           ,(R,VAR(6)),(DEL1,VAR(7)),(DEL1D,VAR(8)),(DEL2,VAR(9)),    SFRC  56
```

```
     2             (DEL2D,VAR(10)),(DEL3,VAR(11)),(DEL3D,VAR(12)),          SFRC  57
     3             (PHIR,VAR(13)),(PHIRD,VAR(14)),(THETTP,VAR(15)),         SFRC  58
     4             (PHITP,VAR(16)),(PSITP,VAR(17)),(XCP,VAR(18)),           SFRC  59
     5             (YCP,VAR(19)),(ZCP,VAR(20)),(PSIFI,VAR(21)),             SFRC  60
     6             (PSIFID,VAR(22))                                         SFRC  61
      EQUIVALENCE (DU,DER(1)),(DV,DER(2)),(DW,DER(3)),(DP,DER(4)),          SFRC  62
     1            (DQ,DER(5)),(DR,DER(6)),(DDEL1,DER(7)),(DDEL1D,DER(8))SFRC  63
     2           ,(DDEL2,DER(9)),(DDEL2D,DER(10)),(DDEL3,DER(11)),         SFRC  64
     3            (DDEL3D,DER(12)),(DPHIR,DER(13)),(DPHIRD,DER(14)),       SFRC  65
     4            (DTHTTP,DER(15)),(DPHITP,DER(16)),(DPSITP,DER(17)),      SFRC  66
     5            (DXCP,DER(18)),(DYCP,DER(19)),(DZCP,DER(20)),            SFRC  67
     6            (DPSIFI,DER(21)),(DDPSFI,DER(22))                        SFRC  68
      DIMENSION YCIP(2)                                                     SFRC  69
      LOGICAL LCB1,LCB2                                                     SFRC  70
      COMMON/INPT2/A4,YBPO,ZBTP,ZBBP,XVF,XVR,YV,ZVT,ZVB,AKV,SIGR(11),SETSFRC  71
     1            ,CONS,AMUB,EPSV,EPSB,XM,EPST,DDD,INDB,DELYBP,            SFRC  72
     2             DELTB, A0, DATDRV(9), XINPT(100)                        SFRC  73
      COMMON/BARIER/FN,IBHIT,JBHIT,XCPNP(3),YCPNP(3),ZCPNP(3),XCPN(3),      SFRC  74
     1              YCPN(3),ZCPN(3),AA1(17),BB1(17),CC1(17),RR1(17),        SFRC  75
     2              AA2(17),BB2(17),CC2(17),RR2(17),CAB,CBB,CGB,CABT,       SFRC  76
     3              CBBT,CGBT,RB,XBT,YBT,ZBT,XBB,YBB,ZBB,RR2P(17),          SFRC  77
     4              YBPT,XNN(17),YNN(17),ZNN(17),XMTX(3,4),IDPT(17),IPT     SFRC  78
     5              ,ININD,UNP(17),VNP(17),WNP(17),VMAX(4),I1,I2,I3,I4,     SFRC  79
     6              XCPTP,YCPTP,ZCPTP,XCPBP,YCPBP,ZCPBP,YCPMP,AINTI,        SFRC  80
     7              AINTP,SXR,SYR,SZR,SDEN,XRI,YRI,ZRI,FRICT,DELBB,VTAN,SFRC  81
     8              FNP,FB,URP,VRP,WRP,EPSL,XLUP,DELX,VL,NCYC,EEE,ENRGY,SFRC  82
     9              SWORK,SPENGY,DISS,IPLN,ILOAD                            SFRC  83
      DIMENSION INDXPT(4)                                                   SFRC  84
      EQUIVALENCE(INDXPT,I1)                                                SFRC  85
      EQUIVALENCE (YCIP,YC1P)                                               SFRC  86
      EQUIVALENCE (XIYP,XTRA(1)),(SPHIC,XTRA(2)),(CPHIC,XTRA(3))            SFRC  87
      EQUIVALENCE(NSEG,XTRA(4))                                             SFRC  88
      EQUIVALENCE (YBPTP,XTRA(7)),(PCAB,XTRA(8)),(PCBB,XTRA(9)),            SFRC  89
     1            (PCGB,XTRA(10)),(PPRB,XTRA(11)),(CAB1,XTRA(12)),         SFRC  90
     2            (CBB1,XTRA(13)),(CGB1,XTRA(14)),(RB1,XTRA(15))           SFRC  91
      EQUIVALENCE(NUNLD,XTRA(16))                                           SFRC  92
      EQUIVALENCE(NLDCTR,XTRA(17))                                          SFRC  93
      EQUIVALENCE (VDEF,XTRA(18)),(PVDEF,XTRA(19))                          SFRC  94
      EQUIVALENCE(PSZR,XTRA(20))                                            SFRC  95
NEW   COMMON/BARSTR/ XSTIO(3),YSTIO(3),ZSTIO(3),XSTI(3),YSTI(3),ZSTI(3),
     1              YSTIPO(3),XSTIP(3),YSTIP(3),ZSTIP(3),FNSTI(3),AKSI(3)
      SFXS = 0.0                                                            SFRC  96
      YBP = 0.0                                                             SFRC  97
      SFYS = 0.0                                                            SFRC  98
      SFZS = 0.0                                                            SFRC  99
      SNPS = 0.0                                                            SFRC 100
      SNTS = 0.0                                                            SFRC 101
      SNPSS = 0.0                                                           SFRC 102
      FN = 0.0                                                              SFRC 103
      IBHIT = 0                                                             SFRC 104
      IPLN = 0                                                              SFRC 105
      NAXIS = 0                                                             SFRC 106
      FRICT = 0.0                                                           SFRC 107
      VTAN = 0.0                                                            SFRC 108
      VMAX(1) = 0.0                                                         SFRC 109
      NSLCE = 0                                                             SFRC 110
      NUNLD=0
      NUNLD2=0  NEW
```

```
      XMTX(2,3) = PCGB                                                  SFRC 168
      XMTX(2,4) = PPRB                                                  SFRC 169
      XMTX(3,1) = 0                                                     SFRC 170
      XMTX(3,2) = 0                                                     SFRC 171
      XMTX(3,3) = 1                                                     SFRC 172
      XMTX(3,4) = PSZR                                                  SFRC 173
      CALL SIMSOL(XMTX,3,3,1)
      XB1 = XMTX(1,4)                                                   SFRC 175
      YB1 = XMTX(2,4)                                                   SFRC 176
      ZB1 = XMTX(3,4)                                                   SFRC 177
      IF (XVR.LE.XB1.AND.XB1.LE.XVF.AND.ABS(YB1).LT.YV.AND.ZVT.LE.ZB1   SFRC 178
     1.AND.ZB1.LE.ZVB) NAXIS = 1                                        SFRC 179
      IF(NAXIS.EQ.0.AND.VDEF.LT.PVDEF.AND.XB1.LT.XVR) GO TO 41          SFRC 180
      TMPA = CBB*PCGB-CGB*PCBB                                          SFRC 181
      TMPB = CGB*PCAB-CAB*PCGB                                          SFRC 182
      TMPC = CAB*PCBB-CBB*PCAB                                          SFRC 183
      TMPAP = TMPB*CGB-TMPC*CBB                                         SFRC 184
      TMPBP =-TMPC*CAB-TMPA*CGB                                         SFRC 185
      TMPCP =-TMPA*CBB-TMPB*CAB                                         SFRC 186
      TMPD = SQRT(TMPAP**2+TMPBP**2+TMPCP**2)                           SFRC 187
      CAB1 = TMPAP/TMPD                                                 SFRC 188
      CBB1 = TMPBP/TMPD                                                 SFRC 189
      CGB1 = TMPCP/TMPD                                                 SFRC 190
      RB1 = XB1*CAB1+YB1*CBB1+ZB1*CGB1                                  SFRC 191
      YB1VF = 1.0E6                                                     SFRC 192
      IF(CBB1.NE.0.) YB1VF=(RB1-XVF*CAB1)/CBB1                          SFRC 193
   78 DO 79 I=12,17                                                     SFRC 194
      AA2(I) = CAB1                                                     SFRC 195
      BB2(I) = CBB1                                                     SFRC 196
      CC2(I) = CGB1                                                     SFRC 197
      RR2(I) = RB1                                                      SFRC 198
   79 CONTINUE                                                          SFRC 199
C PRESENT LOCATION OF HARDPOINTS IN SPACE FIXED COORDINATES
80    DO 81 I=1,3                          (deformed hardpoints)
      XSTIP(I)=XCP+AMTX(1,1)*XSTI(I)+AMTX(1,2)*YSTI(I)+AMTX(1,3)*ZSTI(I)   NEW
      YSTIP(I)=YCP+AMTX(2,1)*XSTI(I)+AMTX(2,2)*YSTI(I)+AMTX(2,3)*ZSTI(I)
      ZSTIP(I)=ZCP+AMTX(3,1)*XSTI(I)+AMTX(3,2)*YSTI(I)+AMTX(3,3)*ZSTI(I)
81    CONTINUE
      XRI=0.
      YRI = 0.0                                                         SFRC 201
      ZRI = 0.0                                                         SFRC 202
      AINTI = 0.0                                                       SFRC 203
      SXR = 0.0                                                         SFRC 204
      SYR = 0.0                                                         SFRC 205
      SZR = 0.0                                                         SFRC 206
      SDEN = 0.0                                                        SFRC 207
      FNX=0.
      FNX1=0.
      FB=0.
      FBFN=0.
      SFNST=0.
      NSEG = (YCPMP-YBPTP)/DELYBP+1.0                                   SFRC 208
      IPLN=NSEG
      YBP=YBPTP+IPLN*DELYBP
      NSG111 = NSEG+1                                                   SFRC 209
      I111 = 1                                                          SFRC 210
    9 DO 38 I=I111,NSG111                                               SFRC 211
      IPLNP=IPLN
```

```
      PYBP=YBP
      PDELBB=DELBB
      PPSXR=SXR
      PPSYR=SYR
      PPSZR=SZR
      PSDEN=SDEN          Store Info. from previous slice
      PFNX=FNX
      PFNX1=FNX1
      PFB=FB
      PFBFN=FBFN
      PSFNST=SFNST
      SFNST=0.
      IPLN = NSEG-I+1                                                    SFRC 212
      YBP = YBPTP+IPLN*DELYBP                                            SFRC 213
      DO 91 IJ=1,3          Compute Force on hardpoint
      FNSTI(IJ)=0.
      IF(YSTIP(IJ).GE.YBP)FNSTI(IJ)=AKST(IJ)*(YSTIPO(IJ)-YBP)
      SFNST=SFNST+FNSTI(IJ)
   91 CONTINUE              based on undeformed position
      IF(YBP.LT.YBPO+EPSL+SET*DELX)GO TO 40                              SFRC 214
      TMP = YBP-YCP                                                      SFRC 215
      XBI = -AMTX(1,1)*XCP+AMTX(2,1)*TMP-AMTX(3,1)*ZCP                   SFRC 216
      YBI = -AMTX(1,2)*XCP+AMTX(2,2)*TMP-AMTX(3,2)*ZCP                   SFRC 217
      ZBI = -AMTX(1,3)*XCP+AMTX(2,3)*TMP-AMTX(3,3)*ZCP                   SFRC 218
      RBI = XBI*CAB+YBI*CBB+ZBI*CGB                                      SFRC 219
      IPT = 0                                                            SFRC 220
   10 DO 15  J=1,17                                                      SFRC 221
      IDPT(J) = 0                                                        SFRC 222
      IF(PSIT.LE.0.0.AND.J.LE.2)GO TO 15                                 SFRC 223
      IF(ININD.LT.2.AND.J.GT.11) GO TO 15                                SFRC 224
      IF(CAB.EQ.0..AND.(J.EQ.4.OR.J.EQ.5.OR.J.EQ.10.OR.J.EQ.11))GO TO 15 SFRC 225
      IF(CBB.EQ.0..AND.(J.LE.2.OR.J.EQ.7.OR.J.EQ.8)) GO TO 15            SFRC 226
      IF(CGB.EQ.0..AND.(J.EQ.3.OR.J.EQ.6.OR.J.EQ.9)) GO TO 15            SFRC 227
      IF(CAB1*CBB.EQ.CBB1*CAB.AND.(J.EQ.12.OR.J.EQ.13)) GO TO 15         SFRC 228
      IF(CBB1*CGB.EQ.CGB1*CBB.AND.(J.EQ.14.OR.J.EQ.15)) GO TO 15         SFRC 229
      IF(CGB1*CAB.EQ.CAB1*CGB.AND.J.GE.16) GO TO 15                      SFRC 230
      IF(NAXIS.EQ.0.AND.J.GT.11) GO TO 15                                SFRC 231
   11 XMTX(1,1) = CAB                                                    SFRC 232
      XMTX(1,2) = CBB                                                    SFRC 233
      XMTX(1,3) = CGB                                                    SFRC 234
      XMTX(1,4) = RBI                                                    SFRC 235
   12 XMTX(2,1) = AA1(J)                                                 SFRC 236
      XMTX(2,2) = BB1(J)                                                 SFRC 237
      XMTX(2,3) = CC1(J)                                                 SFRC 238
      XMTX(2,4) = RR1(J)                                                 SFRC 239
   13 XMTX(3,1) = AA2(J)                                                 SFRC 240
      XMTX(3,2) = BB2(J)                                                 SFRC 241
      XMTX(3,3) = CC2(J)                                                 SFRC 242
      XMTX(3,4) = RR2(J)                                                 SFRC 243
   14 CALL SIMSOL(XMTX,3,3,2)
      XNN(J) = XMTX(1,4)                                                 SFRC 245
      YNN(J) = XMTX(2,4)                                                 SFRC 246
      ZNN(J) = XMTX(3,4)                                                 SFRC 247
      IF(XNN(J).LT.XVR.OR.XNN(J).GT.XVF) GO TO 15                        SFRC 248
      IF(ABS(YNN(J)).GT.YV) GO TO 15                                     SFRC 249
      IF(ZNN(J).LT.ZVT.OR.ZNN(J).GT.ZVB) GO TO 15                        SFRC 250
      IDPT(J) = 1                                                        SFRC 251
      IPT = IPT+1                                                        SFRC 252
```

NEW

NEW

```
      IPPT = J                                                          SFRC 253
   15 CONTINUE                                                          SFRC 254
      IF(IPPT.LE.11.AND.(NAXIS.EQ.1.AND.YB1VF.GT.YV.AND.ININD.EQ.2))    SFRC 255
     1 GO TO 38                                                         SFRC 256
      IF(MOD(INDB,2).EQ.0) GO TO 23                                     SFRC 257
      IF(CGB.EQ.0.0.AND.CGBT.EQ.0.0)GO TO 23                            SFRC 258
      RR2P(1) = RBT                                                     SFRC 259
      RR2P(2) = RBB                                                     SFRC 260
      RR2P(4) = RBT                                                     SFRC 261
      RR2P(5) = RBB                                                     SFRC 262
      RR2P(7) = RBT                                                     SFRC 263
      RR2P(8) = RBB                                                     SFRC 264
      RR2P(10) = RBT                                                    SFRC 265
      RR2P(11) = RBB                                                    SFRC 266
      RR2P(12) = RBT                                                    SFRC 267
      RR2P(13) = RBB                                                    SFRC 268
      RR2P(14) = RBT                                                    SFRC 269
      RR2P(15) = RBB                                                    SFRC 270
      RR2P(16) = RBT                                                    SFRC 271
      RR2P(17) = RBB                                                    SFRC 272
   16 DO 22  J=1,17                                                     SFRC 273
      IF(PSIT.LE.0.0.AND.J.LE.2)GO TO 22                                SFRC 274
      IF(J.EQ.3.OR.J.EQ.6.OR.J.EQ.9) GO TO 22                           SFRC 275
      IF(CAB*CGBT.EQ.CGB*CABT.AND.(J.EQ.4.OR.J.EQ.5.OR.J.EQ.10.OR.      SFRC 276
     1   J.EQ.11)) GO TO 22                                             SFRC 277
      IF(CGB*CBBT.EQ.CBB*CGBT.AND.(J.LE.2.OR.J.EQ.7.OR.J.EQ.8)) GO TO 22SFRC 278
      IF(CAB*(CBB1*CGBT-CBBT*CGB1)-CAB1*(CBB*CGBT-CBBT*CGB)+CABT*(CBB*  SFRC 279
     1   CGB1-CBB1*CGB).EQ.0.0.AND.J.GE.12) GO TO 22                    SFRC 280
      IF(J.GE.12.AND.IDPT(J).NE.1) GO TO 22                             SFRC 281
      IF(IDPT(1).EQ.1.AND.IDPT(2).EQ.1.AND.J.EQ.14) GO TO 173           SFRC 282
      IF(IDPT(7).EQ.1.AND.IDPT(8).EQ.1.AND.J.EQ.15) GO TO 173           SFRC 283
      IF(IDPT(4).EQ.1.AND.IDPT(5).EQ.1.AND.J.EQ.16) GO TO 173           SFRC 284
      IF(IDPT(10).EQ.1.AND.IDPT(11).EQ.1.AND.J.EQ.17) GO TO 173         SFRC 285
      XMTX(1,1) = CAB                                                   SFRC 286
      XMTX(1,2) = CBB                                                   SFRC 287
      XMTX(1,3) = CGB                                                   SFRC 288
      XMTX(1,4) = RBI                                                   SFRC 289
      IF(J.GE.12) GO TO 170                                             SFRC 290
      XMTX(2,2) = BB1(J)                                                SFRC 291
      XMTX(2,3) = CC1(J)                                                SFRC 292
   17 XMTX(2,1) = AA1(J)                                                SFRC 293
      XMTX(2,4) = RR1(J)                                                SFRC 294
      GO TO 18                                                          SFRC 295
  170 XMTX(2,1) = AA2(J)                                                SFRC 296
      XMTX(2,2) = BB2(J)                                                SFRC 297
      XMTX(2,3) = CC2(J)                                                SFRC 298
      XMTX(2,4) = RR2(J)                                                SFRC 299
   18 XMTX(3,1) = CABT                                                  SFRC 300
      XMTX(3,2) = CBBT                                                  SFRC 301
      XMTX(3,3) = CGBT                                                  SFRC 302
      IF((IDPT(1).EQ.1.AND.J.EQ.14).OR.(IDPT(4).EQ.1.AND.J.EQ.16))      SFRC 303
     1 GO TO 171                                                        SFRC 304
      IF((IDPT(8).EQ.1.AND.J.EQ.15).OR.(IDPT(11).EQ.1.AND.J.EQ.17))     SFRC 305
     1 GO TO 172                                                        SFRC 306
      XMTX(3,4) = RR2P(J)                                               SFRC 307
      GO TO 19                                                          SFRC 308
  171 XMTX(3,4) = RBB                                                   SFRC 309
      GO TO 19                                                          SFRC 310
```

```
  172 XMTX(3,4) = RBT                                                    SFRC 311
19    CALL SIMSOL(XMTX,3,3,3)
      IF(XMTX(1,4).LT.XVR.OR.XMTX(1,4).GT.XVF) GO TO 22                  SFRC 313
      IF(ABS(XMTX(2,4)).GT.YV) GO TO 22                                  SFRC 314
      IF(XMTX(3,4).LT.ZVT.OR.XMTX(3,4).GT.ZVB) GO TO 22                  SFRC 315
      IF(IDPT(J).NE.0) GO TO 20                                          SFRC 316
      IDPT(J) = 1                                                        SFRC 317
      GO TO 21                                                           SFRC 318
   20 IF(ABS(XMTX(3,4)).GE.ABS(ZNN(J)))GO TO 22                          SFRC 319
   21 XNN(J) = XMTX(1,4)                                                 SFRC 320
      YNN(J) = XMTX(2,4)                                                 SFRC 321
      ZNN(J) = XMTX(3,4)                                                 SFRC 322
      GO TO 22                                                           SFRC 323
  173 IDPT(J) = 0                                                        SFRC 324
      IPT = IPT-1                                                        SFRC 325
   22 CONTINUE                                                           SFRC 326
   23 IF(IPT.LT.3) GO TO 38                                              SFRC 327
   24 DO 25  J=1,17                                                      SFRC 328
      IF(IDPT(J).EQ.0) GO TO 25                                          SFRC 329
      TMPU = U-YNN(J)*R+ZNN(J)*Q                                         SFRC 330
      TMPV = V+XNN(J)*R-ZNN(J)*P                                         SFRC 331
      TMPW = W+YNN(J)*P-XNN(J)*Q                                         SFRC 332
      UNP(J) = AMTX(1,1)*TMPU+AMTX(1,2)*TMPV+AMTX(1,3)*TMPW              SFRC 333
      VNP(J) = AMTX(2,1)*TMPU+AMTX(2,2)*TMPV+AMTX(2,3)*TMPW              SFRC 334
      WNP(J) = AMTX(3,1)*TMPU+AMTX(3,2)*TMPV+AMTX(3,3)*TMPW              SFRC 335
   25 CONTINUE                                                           SFRC 336
   26 DO 27  J=1,4                                                       SFRC 337
      VMAX(J) = -1.0E30                                                  SFRC 338
      INDXPT(J) = 0                                                      SFRC 339
   27 CONTINUE                                                           SFRC 340
   28 DO 34  J=1,17                                                      SFRC 341
      IF(IDPT(J).EQ.0) GO TO 34                                          SFRC 342
   29 DO 33  K=1,4                                                       SFRC 343
      IF(VNP(J).LT.VMAX(K)) GO TO 33                                     SFRC 344
      IF(K.EQ.4) GO TO 32                                                SFRC 345
      K1 = K+1                                                           SFRC 346
   30 DO 31  L=K1,4                                                      SFRC 347
      M = 4-L+K1                                                         SFRC 348
      VMAX(M) = VMAX(M-1)                                                SFRC 349
      INDXPT(M) = INDXPT(M-1)                                            SFRC 350
   31 CONTINUE                                                           SFRC 351
   32 VMAX(K) = VNP(J)                                                   SFRC 352
      INDXPT(K) = J                                                      SFRC 353
      GO TO 34                                                           SFRC 354
   33 CONTINUE                                                           SFRC 355
   34 CONTINUE                                                           SFRC 356
      IPT = 4                                                            SFRC 357
      IF(INDXPT(4).EQ.0) IPT = 3                                         SFRC 358
   37 J3 = I3                                                            SFRC 359
      J1 = I1                                                            SFRC 360
      J2 = I2                                                            SFRC 361
      J4 = I4                                                            SFRC 362
      CALL AREA                                                          SFRC 363
      IF(IB.EQ.1) GO TO 38                                               SFRC 364
      FNX1=AKV*DELYBP*SDEN
      FNX=FNX1+SFNST
      IF(NSLCE.NE.0) GO TO 38                                            SFRC 366
   40 DELBB = AMAX1(YBP-YBPO,EPSL+SET*DELX)                              SFRC 367
```

```
      CALL NLDFRC                                                    SFRC 368
      FBFN=FB-FNX
      IF(EPSB.LT.FBFN)GOTO38
      IF(I.EQ.1)GOTO105
      IF(FBFN.GE.0.)GOTO105
      IF(ABS(FBFN).LT.ABS(PFBFN))GOTO105
      PRINT 1001,T,I,YBP,PYBP,FNX,PFNX
1001  FORMAT(T2,' T=',F7.4,' I=',I3,' YBP=',F10.4,' PYBP=',F10.4,' FNX='
     1,G13.5,' PFNX=' ,G13.5,' EQUILIB AT PREV SLICE RESET')
      IPLN=IPLNP
      YBP=PYBP
      DELBB=PDELBB        Previous Slice had better Equilibrium
      SXR=PPSXR           ∴ reset values
      SYR=PPSYR
      SZR=PPSZR
      SDEN=PSDEN
      FNX=PFNX
      FNX1=PFNX1
      FB=PFB
      SFNST=PSFNST
105   YBPT=AMAX1(YBP,YBPO+EPSL+SET*DELX)
      NSLCE = NSLCE+1                                                SFRC 371
      IF(NLDCTR.EQ.3)CALL NLDFL                                      SFRC 372
      NUNLD2=0
      IF(NUNLD.EQ.0)GOTO38
      NUNLD2=1
      GOTO110
38    CONTINUE
110   DO 111 IJ=1,3
      IF(YSTIP(IJ).GT.YBPT)YSTIP(IJ)=YBPT   Compute Position of
      AA=XSTIP(IJ)-XCP                      deformed hardpoints in
      BB=YSTIP(IJ)-YCP                      vehicle-fixed coordinates
      CC=ZSTIP(IJ)-ZCP
      XSTI(IJ)=AMTX(1,1)*AA+AMTX(2,1)*BB+AMTX(3,1)*CC
      YSTI(IJ)=AMTX(1,2)*AA+AMTX(2,2)*BB+AMTX(3,2)*CC
      ZSTI(IJ)=AMTX(1,3)*AA+AMTX(2,3)*BB+AMTX(3,3)*CC
111   CONTINUE
      IF(NUNLD2.NE.0)GOTO103
      IF(NUNLD.NE.0) GO TO 100                                       SFRC 375
      IF( IB .NE. 1)  GO TO 50                                       SFRC 376
   45 NEGPT=0                                                        SFRC 377
      DO 46  J=1,IPT                                                 SFRC 378
      IF( VMAX(J) .LT.  0.0 )  NEGPT=NEGPT + 1                       SFRC 379
   46 CONTINUE                                                       SFRC 380
      IF( NEGPT .GE. IPT) GO TO 41                                   SFRC 381
50    FN =AKV*DELYBP*SDEN
      FN1=FN +SFNST
      IF(ININD.EQ.0) ININD = 1                                       SFRC 383
      IF(FN1.NE.0.0.AND.NUNLD.EQ.0) CALL RESFRC
      IF(NSLCE.EQ.0.AND.IB.EQ.1) GO TO 103                           SFRC 385
      IF(NSLCE.EQ.0) GO TO 100                                       SFRC 386
  103 TMP = YBPT-YCP                                                 SFRC 387
      NUNLD2=0
      XBPP = -AMTX(1,1)*XCP+AMTX(2,1)*TMP-AMTX(3,1)*ZCP              SFRC 388
      YBPP = -AMTX(1,2)*XCP+AMTX(2,2)*TMP-AMTX(3,2)*ZCP              SFRC 389
      ZBPP = -AMTX(1,3)*XCP+AMTX(2,3)*TMP-AMTX(3,3)*ZCP              SFRC 390
      RB = XBPP*CAB + YBPP*CBB + ZBPP*CGB                            SFRC 391
      GO TO 39                                                       SFRC 392
```

NEW

NEW

```
  100 NUNLD = NUNLD+1                                                    SFRC 393
      NSG111 = NSG111+1                                                  SFRC 394
      I111 = NSG111                                                      SFRC 395
      GO TO 9                                                            SFRC 396
   39 NUNLD = 0                                                          SFRC 397
   41 IF(NLDCTR.EQ.3.AND.IPT.GE.3)WRITE(6,1000)T,XB1,YB1,IPT,J1,J2,J3,   SFRC 398
     1         J4,XNN(J1),YNN(J1),ZNN(J1),XNN(J2),YNN(J2),ZNN(J2),      SFRC 399
     2            XNN(J3),YNN(J3),ZNN(J3),XNN(J4),YNN(J4),ZNN(J4)       SFRC 400
 1000 FORMAT(F7.4,2F7.1,5I3,12F8.1)                                      SFRC 401
      NLDCTR = NLDCTR+1                                                  SFRC 402
      RETURN                                                             SFRC 403
      END                                                                SFRC 404
```

```
OMPILER OPTIONS - NAME=  MAIN,OPT=02,LINECNT=60,SOURCE,EBCDIC,NOLIST,NODECK,LOAD,MAP,N
    C     SINGLE VEHICLE ACCIDENT SIMULATION - SUBROUTINE RESFRC                RSFR   0
          SUBROUTINE RESFRC                                                     RSFR   1
          COMMON/INPT/PHIO,THETAO,PSIO,PO,QO,RO,XCOP,YCOP,ZCOP,UO,VO,WO,A,B,RSFR   2
         1            DEL1O,DEL2O,DEL3O,PHIRO,DEL1OD,DEL2OD,DEL3OD,PHIROD,TFRSFR   3
         2           ,TR,ZF,ZR,RHO,RW,AKT,SIGT,XLAMT,A1,A2,A3,AKRS,AMU,XMUR,RSFR   4
         3            XMS,XMUF,XIX,XIY,XIZ,XIXZ,CF,AKF,XLAMF,OMEGF,CFP,EPSF,RSFR   5
         4            RF,CR,AKR,XLAMR,OMEGR,CRP,EPSR,RR,TS,THMAX,DTCOMP,TO,  RSFR   6
         5            T1,DTCMP1,DTPRNT,MODE,EBAR,EM,AAA,HMAX,HMIN,BET,G,     RSFR   7
         6            HED(36),DADE(3),XIR,X1,Y1,Z1,X2,Y2,Z2,PHIC(50),DELB,   RSFR   8
         7            DELE,DDEL,NDEL,PSIF(50),TQF(50),TQR(50),TB,TE,TINCR,   RSFR   9
         8            XBDRY(10),YBDRY(10),ZGP(21,21),THG(21,21),PHIG(21,21),RSFR  10
         9            XB,XE,XINCR,NX,YB,YE,YINCR,NY,NBX,NBY,UVWMIN,PQRMIN    RSFR  11
          COMMON/INPT1/YC1P,YC2P,ZC2P,DELTC,PHIC1,PHIC2,AMUC,FJP(35),XIPS,      RSFR  12
         1             CPSP,OMGPS,AKPS,EPSPS,XPS,RWHJB,RWHJE,DRWHJ,INDCRB,    RSFR  13
         2             PSIFIO,PSIFDO                                          RSFR  14
          COMMON /INTG/NEQ,T,DT,VAR(50),DER(50)                                 RSFR  15
          COMMON /DIMV/X1P,X2P,X3P,X4P,Y1P,Y2P,Y3P,Y4P,Z1P,Z2P,Z3P,Z4P,PHI1,RSFR  16
         1             PHI2,PHI3,PHI4,PSI1,PSI2,PSI3,PSI4,CAYW(4),CBYW(4),    RSFR  17
         2             CGYW(4),ZPGI(4),THGI(4),PHGI(4),CPG(4),SPG(4),CTG(4),RSFR  18
         3             STG(4),CAGZ(4),CBGZ(4),CGGZ(4),D1(4),D2(4),D3(4),      RSFR  19
         4             XLM1(4),XLM2(4),XLM3(4),AMTX(3,3),CMTX(3,4),XGPP(4),   RSFR  20
         5             YGPP(4),ZGPP(4),DMATX(10,11),DELTA(4),CAR(4),CBR(4),   RSFR  21
         6             CGR(4),FR(4),HI(4),FC(4),TI(4),AX(4),BX(4),CX(4),      RSFR  22
         7             CTXG(4),UG(4),STXG(4),AY(4),BY(4),CY(4),CPYG(4),       RSFR  23
         8             SPYG(4),VG(4),PSIIP(4),PHICI(4),CAC(4),CBC(4),CGC(4),RSFR  24
         9             FCXU(4),FCYU(4),FCZU(4),FS(4),CAXW(4),CBXW(4),CGXW(4)RSFR  25
          COMMON /DIMV/AS(4),BS(4),CS(4),CAS(4),CBS(4),CGS(4),BETP(4),       RSFR  26
         1             BETBR(4),FSXU(4),FSYU(4),FSZU(4),FRXU(4),FRYU(4),      RSFR  27
         2             FRZU(4),FXU(4),FYU(4),FZU(4),SI(4),F1FI(2),F1RI(2),    RSFR  28
         3             F2FI(2),F2RI(2),CAH(4),CBH(4),CGH(4)                   RSFR  29
          COMMON /COMP/SUMM,THETN,PHIN,PSIN,PI,RAD,GAM1,GAM2,GAM3,GAM4,GAM5,RSFR  30
         1             GAM6,GAM7,GAM8,GAM9,THETT,PHIT,PSIT,A12,A23,ZRO,TRO2,RSFR  31
         2             TFO2,TIZ,RHO2,RHOMUR,AMUF,BMUR,ZPR,TM4,RHMR2,AO2APB,   RSFR  32
         3             BO2APB,RFTF,TSO2,RRTS,BROMUR,XMUFO2,AXMFO2,XMTFO4,     RSFR  33
         4             XIZR,RTR,RHMR2I,XIXP,XIZP,XIXZP,XIYZP,D1PD2,D1MD2,     RSFR  34
         5             ZRD3,ZRD3R,ZFD3R,ZFD12,TIZ2,TG61,DD1P2,DD1M2,RPR,PHRPRSFR  35
         6            ,TANTP,SPHTP,CPHTP,SECTP,SFXS,SFYS,SFZS,SNPS,SNTS,      RSFR  36
         7             SNPSS,TPR,CAY,CBY,CGY,CAX,CBX,CGX,SFYU,SFXU,SFYUF,     RSFR  37
         8             SFYUR,SFZU,COSTH,SINTH,COSPS,SINPS,COSPH,SINPH,ANG1,   RSFR  38
         9             ANG2,CPHI,SPHI,CPSI,SPSI,P1,P7,P3,P4,P5,P6,TX,TY,TZ    RSFR  39
          COMMON /COMP/TRH,DISTX,DISTY,DISTD,DISTS,D21,ZETA4,ZETA4D,ZETA3,   RSFR  40
         1             ZETA3D,SFZ1,SNPU,SNTU,HCGH1,HCGH2,HCGH3,HCGH4,TERM1,   RSFR  41
         2             TERM2,SNPSU,SNPR,HCBH1,HCBH2,HCBH3,HCBH4,HCAH1,HCAH2,RSFR  42
         3             HCAH3,HCAH4,UQ,WP,UR,QR,VP,PR,P2,Q2,R2,VR,WQ,PQ,PHIR2RSFR  43
         4            ,PHIRD2,RPHRD,GCTH,GSTH,GCTSP,GCTCP,XXX,YYY,IX,IY,XX1,RSFR  44
         5             XX2,YY1,YY2,THG1,THG2,PHG1,PHG2,ZZ1,ZZ2,LLL            RSFR  45
          COMMON /COMPN/ OMT2M1,FRSP(4),FRCP(4),OMEGT,ICBHIT,JCBHIT,         RSFR  46
         1               DPSINT,TANPC1,TANPC2,PHIC1R,PHIC2R,AMUCMP,PHI1D,    RSFR  47
         2               PHI2D,LCB1(4),LCB2(4),IHIT,AJMTX(3,3),BMTX(3,3),    RSFR  48
         3               SFRX(4),SFRY(4),SFRZ(4),T1PSI,T2PSI,XMU             RSFR  49
          COMMON/ADTNL/U1,U2,U3,U4,V1,V2,V3,V4,W1,W2,W3,W4,XTRA(300)          RSFR  50
          DIMENSION XP(4),YP(4),ZP(4),PHII(4),PSII(4),UI(4),VI(4),WI(4)      RSFR  51
          EQUIVALENCE (XP,X1P),(YP,Y1P),(ZP,Z1P),(PHII,PHI1),(PSII,PSI1),    RSFR  52
         1            (UI,U1),(VI,V1),(WI,W1)                               RSFR  53
          EQUIVALENCE (U,VAR(1)),(V,VAR(2)),(W,VAR(3)),(P,VAR(4)),(Q,VAR(5))RSFR  54
         1           ,(R,VAR(6)),(DEL1,VAR(7)),(DEL1D,VAR(8)),(DEL2,VAR(9)),RSFR  55
         2            (DEL2D,VAR(10)),(DEL3,VAR(11)),(DEL3D,VAR(12)),       RSFR  56
         3            (PHIR,VAR(13)),(PHIRD,VAR(14)),(THETTP,VAR(15)),      RSFR  57
```

```
      VTAN=SQRT(URP*URP+WRP*WRP)
      TEMP1=0.
      TEMP2=0.
      IF(VTAN.LT.EPSV)GOTO6
      AA=AMUB*FN
      FRICT=AA
      AA=AA/VTAN
      TEMP1=-AA*URP
      TEMP2=-AA*WRP
6     CONTINUE
      DO5J=1,4
      FX=AMTX(1,1)*TEMP1-AMTX(2,1)*F(J)+AMTX(3,1)*TEMP2
      FY=AMTX(1,2)*TEMP1-AMTX(2,2)*F(J)+AMTX(3,2)*TEMP2
      FZ=AMTX(1,3)*TEMP1-AMTX(2,3)*F(J)+AMTX(3,3)*TEMP2
      TEMP1=0.
      TEMP2=0.
      SFXS=SFXS+FX
      SFYS=SFYS+FY
      SFZS=SFZS+FZ
      SNPS=SNPS+FZ*Y(J)-FY*Z(J)
      SNTS=SNTS+FX*Z(J)-FZ*X(J)
5     SNPSS=SNPSS+FY*X(J)-FX*Y(J)
      RETURN                                                    RSFR 108
      END                                                       RSFR 109
```

Magnitude and Direction of Friction Force

Components of each Force in vehicle-fixed Coordinates

Summing all Forces

Computing and Summing Moments

REVISED

APPENDIX C

ACCELEROMETER LOCATIONS

Vehicle Dimensions - 1963 Plymouth

Weight - 4000 lb
Length - 16'-11" = 203"
Width - 6'-2" = 74"
Wheel base - 9'-8" = 116"
Track width - 5' = 60"
Bumper to front wheel center - 2'-8" = 32"
Front bumper to center of gravity - 7'-7 1/2" = 91 1/2"

Location of accelerometers on frame members (symmetrical about vehicle centerline)

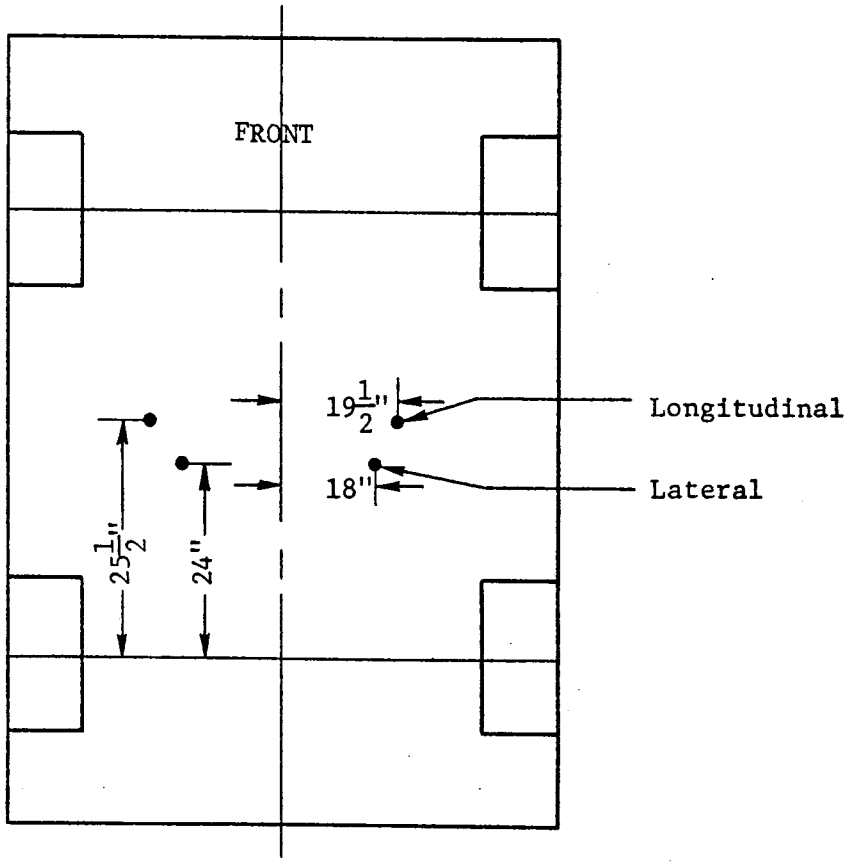

FIGURE C1- Vehicle data for test impacting concrete median barrier at 63 mph at 25 deg.

Vehicle Dimensions - 1963 Chevrolet

Weight - 4210 lb
Length - 17'-3" = 207"
Width - 6'-6" = 78"
Wheel base - 9'-11" = 119"
Track width - 4'-11" = 59"
Bumper to front wheel center - 2'-8" = 32"
Bumper to center of gravity - 7'-2" = 86"

Location of accelerometers on frame members (symmetrical about vehicle centerline)

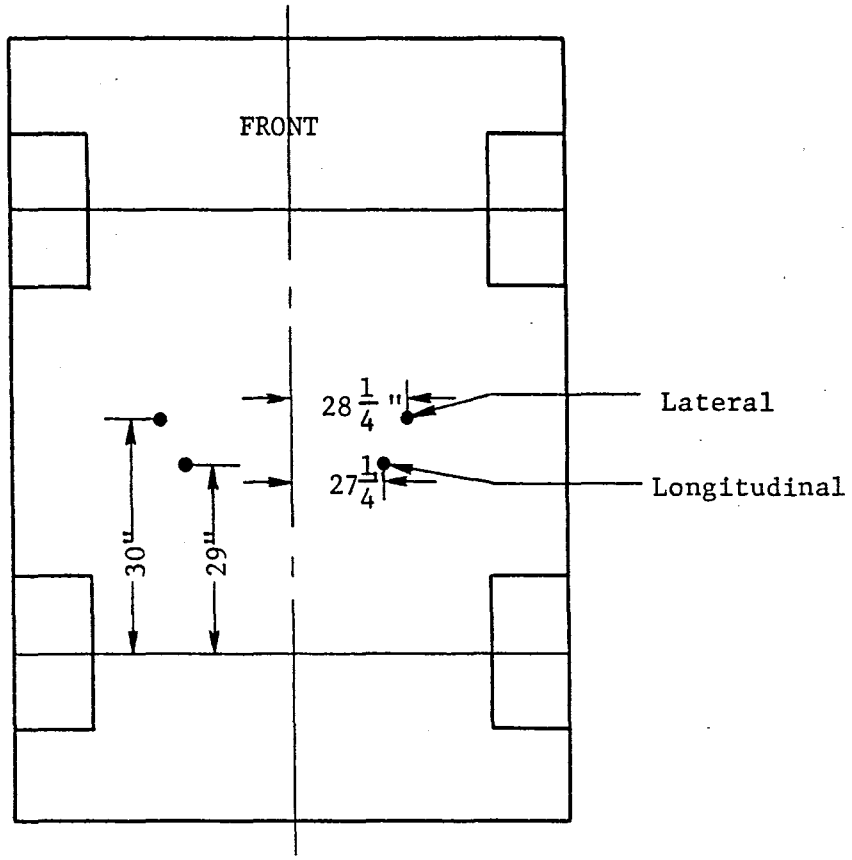

FIGURE C2- Vehicle data for tests impacting concrete median barrier at 61.9 mph at 7 deg, and at 59.6 mph at 15 deg.

APPENDIX D

SEVERITY INDEX

SEVERITY INDEX

An automobile acceleration severity-index was used in this study to quantify the relative severity an automobile impacting a traffic barrier. The severity-index takes into consideration the combined effects of the longitudinal, lateral, and vertical accelerations of the automobile at its center-of-mass. The severity-indes (SI) is computed by Eq. D1.

$$SI = \sqrt{\left(\frac{G_{LONG}}{G_{XL}}\right)^2 + \left(\frac{G_{LAT}}{G_{YL}}\right)^2 + \left(\frac{G_{VERT}}{G_{ZL}}\right)^2} \qquad \text{(D1)}$$

The terms in the numerator of Eq. D1 are the computed or measured accelerations of the automobile; whereas, the terms in the denominator are automobile accelerations which represent a "limiting condition" for the occupant.

An indepth discussion of the background and development of Eq. D1 was given in TTI Research Report 140-4 (7). Information relating tolerable accelerations to degree of occupant restraint, rate of onset or rise time, and time duration of accelerations was included in the discussion. In the study presented herein, the tolerable accelerations were for an unrestrained occupant, rise times greater than 0.03 seconds, and for a time duration of 0.050 seconds. The limit or tolerable accelerations for these conditions are (10):

$$\left.\begin{aligned} G_{XL} &= 7 \text{ G's} \\ G_{YL} &= 5 \text{ G's} \\ G_{ZL} &= 6 \text{ G's} \end{aligned}\right\} \qquad \text{(D2)}$$

There has been much discussion as to the relationship of the severity-index to the probable level of occupant injury. The writers have interpreted an SI of unity to imply that occupants will sustain injuries which border on the "serious" type. Until more data are available on limit accelerations and the interaction relationship itself, there appears to be no other logical way to interpret the index.

In addition, vehicle accelerations have never been translated into expected g-levels on the occupant, and until such a correlation becomes available the possible applications of the severity-index must be qualified. The index in its present form is intended for comparing the severity of one event to another and can also serve as an aide in making decisions concerning highway modifications which should effect a reduction in occupant injury and loss of life. However, it must be emphasized that the index, as defined by TTI researchers (here and elsewhere), has never been intended for direct assessment of human injury and therefore should not be used in that regard.

APPENDIX E

FORMULAS FOR MAXIMUM ROLL ANGLE

VALUES OBTAINED FROM PROGRAM AT TIME OF ITS TERMINATION

Z' (IN), ϕ (DEG), $\dot{\phi}$ (DEG/SEC)

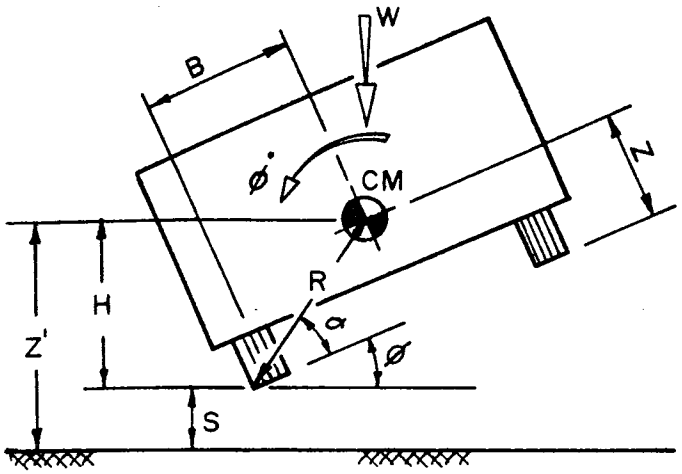

$\alpha = \tan^{-1}(Z/B)$

$R = Z / \sin\alpha$

$H = R \sin(\alpha+\phi)$

$S = Z' - H$

ASSUMPTIONS

1. NEGLECT PITCH ANGLE AND PITCH RATE
2. NO VERTICAL VELOCIY (Z'= MAX)

FIGURE B IA. AUTO AIRBORNE

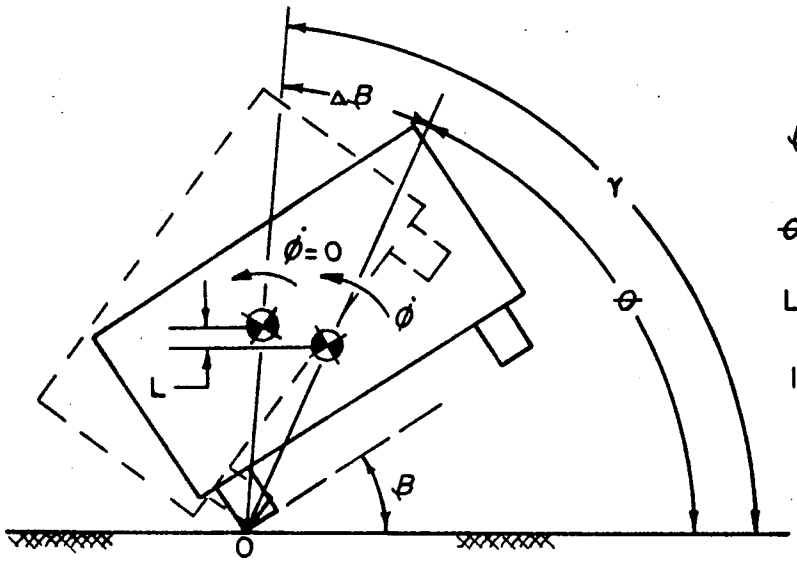

$$\beta = \phi + \sqrt{\frac{2S}{g}}\,\dot{\phi}$$

$\theta = \beta + \alpha$

$L = R(\sin\gamma - \sin\theta)$

$I_O = I_{CM} + \frac{W}{g}R^2$

FIGURE B IB. MAXIMUM ROLL

KINETIC ENERGY = WORK DONE BY AUTO WEIGHT

$$\frac{1}{2} I_O(\dot{\phi})^2 = WL = WR(\sin\gamma - \sin\theta)$$

$$\gamma = \sin^{-1}\left[\frac{1}{2}\frac{I_O\dot{\phi}^2}{WR} + \sin\theta\right]$$

MAX ROLL = $\beta + \Delta\beta$

MAX ROLL = $\beta + \gamma - \theta$

IF: $\gamma > 90°$ ROLLOVER WILL OCCUR

IF: $\beta > 90° - \tan^{-1}(Z/B)$ ROLLOVER WILL OCCUR

FIGURE BI. PROCEDURE TO ESTIMATE MAXIMUM ROLL ANGLE

APPENDIX F

REFERENCES

APPENDIX F

References

1. McHenry, R. R., Segal, D. J., "Determination of Physical Criteria for Roadside Energy Conversion Systems", CAL No. VJ-2251-V-1, Buffalo, N.Y., July, 1967.

2. McHenry, R. R., and Deleys, N. H., "Vehicle Dynamics in Single Vehicle Accidents: Validation and Extensions of a Computer Simulation", CAL No. VJ-2251-V-3, Buffalo, N.Y., December, 1968.

3. Hirsch, T. J., Hayes, G. G., and Post, E. R., "Vehicle Crash Test and Evaluation of Median Barriers for Texas Highways", Research Report No. 146-4, Texas Transportation Institute, College Station, Texas, June, 1972, 1st draft.

4. Young, R. D., Post, E. R., Ross, H. E., Jr., "Simulation of Vehicle Impact with the Texas Concrete Median Barrier - Volume II: Computer Input Data", Research Report 140-5, Texas Transportation Institute, College Station, Texas (in writing).

5. Theiss, C. M., "Perspective Picture Output for Automobile Dynamics Simulation", CAL. No. VJ-2251-V-2R, Cornell Aeronautical Laboratory Inc., Buffalo, New York, January 1969.

6. Deleys, N. J., McHenry, R. R., "Highway Guardrails - A Review of Current Practice", National Cooperative Highway Research Program, Research Report 36, 1967, p. 7.

7. Young, R. D., "A Three Dimensional Mathematical Model of an Automobile Passenger", Research Report 140-2, Texas Transportation Institute, College Station, Texas, August 1970.

8. Young, R. D., Edwards, T. C., Bridwell, R. J., and Ross, H. E., Jr., "Documentation of Input for the Single Vehicle Accident Computer Program", Research Report 140-1, Texas Transportation Institute, College Station, Texas, July, 1969.

9. Ross, H. E., Jr., Post, E. R., "Criteria for Guardrail Need and Location on Embankments - Volume I: Development of Criteria", Research Report 140-4, Texas Transportation Institute, College Station, Texas, April, 1972.